UNIVERSITY *of York*

Discussion Papers in Economics

No. 17/10

European spreads at the interest rate lower bound

Laura Coroneo
Sergio Pastorello

Department of Economics and Related Studies
University of York
Heslington
York, YO10 5DD

European spreads at the interest rate lower bound*

Laura Coroneo
University of York

Sergio Pastorello
University of Bologna

First draft: 26th May 2017
Current draft: 18th September 2017

Abstract

This paper analyzes the effect of the interest rate lower bound on long term sovereign bond spreads in the Euro area. We specify a joint shadow rate term structure model for the risk-free, the German and the Italian sovereign yield curves. In our model, the behavior of long term spreads becomes strongly nonlinear in the underlying factors when interest rates are close to the lower bound, which in the data occurs since the beginning of 2012. We fit the model by Quasi-Maximum Likelihood and highlight three important consequences of sovereign spreads' nonlinear behavior: i) their distribution is skewed, ii) they are affected by (possibly exogenous) changes in the lower bound, and iii) they become less informative about the countries' sovereign risk. Shadow spreads, however, still provide reliable information.

Keywords: lower bound; sovereign risk; shadow rate term structure model.
JEL classification: E43, E44, E52, G12.

*We thank Adam Golinski, Laura Jackson-Young, Tomi Kortela, Ahn Le, Wolfgang Lemke, Attanasios Orphanides, Guillaume Roussellet, Peter Spencer, Dora Xia and participants to the 49^{th} Money, Macro and Finance Research Group Annual Conference, the 2017 International Conference in Computational Economics and Finance, the 8^{th} Macro-Money-Finance Workshop (RCEA), 2016 Asset Pricing Workshop (University of York) and the 2016 Fiscal Policy Symposium (University of York) for helpful comments. Laura Coroneo gratefully acknowledges the support of the ESRC grant ES/K001345/1.

1 Introduction

Long term sovereign bond spreads are closely monitored by financial markets, central banks and governments as a reference measure for sovereign risk. According to standard finance theory, long term rates are determined by the current and expected future short term rates plus a risk premium, i.e. by the current forward curve. Consequently, a lower bound constraining forward sovereign rates will also affect long term sovereign rates, and long term sovereign bond spreads as well.

The existence of a lower bound on interest rates can be justified both theoretically and empirically. Black (1995) was the first to observe that interest rates cannot decrease below the opportunity cost of holding currency, which represents a lower bound on interest rates. This remark implies that standard Gaussian affine dynamic term structure models are misspecified when observed yields are close to that bound, because they assign a large probability to rates below it. Empirically, this situation has become relevant in several countries: in Japan since the late 90s, in the US since 2009 and in the Euro area since 2012.

Several authors suggested that shadow rate term structure models can be used to enforce a lower bound on interest rates, see Krippner (2013), Wu and Xia (2016) and Christensen and Rudebusch (2014), among others. These works show that shadow rate term structure models fit observed yields better than Gaussian affine dynamic term structure models, and offer several advantages in times when rates are constrained from below. Some efforts have also been devoted to highlight the implications of the lower bound on long term yields. In the context of a shadow rate term structure model, Krippner (2015) and Bauer and Rudebusch (2016) measure how tightly the zero lower bound constrains the entire term structure of interest rates using the zero lower bound wedge, defined as the difference between the 10-year yield and the corresponding shadow yield, i.e. the yield that would be observed if interest rates were not constrained. Ruge-Murcia (2006) shows that, at the lower bound, long term rates respond asymmetrically to changes in the short term rate, and by less than it is predicted by a Gaussian affine dynamic term structure model. Swanson and Williams (2014) measure the tightness of the zero lower bound on medium and long term interest rates using the interest rate sensitivity to macroeconomic news.

In this paper, we focus on the effect of the interest rate lower bound on long term sovereign bond spreads. To this end, we specify a joint shadow rate term structure model for a risk-free and two country yield curves in a monetary union. Our model allows for common and country-specific factors, and also for a time varying lower bound. In this framework, observed sovereign spreads can be decomposed in two components: the shadow spread and the spread wedge. The shadow spread is linear in the state variables and represents the unconstrained sovereign spread, i.e. the sovereign spread that we would observe in the absence of a lower bound or if interest rates were far from it. For this reason, the shadow spread is only determined by the sovereign risk. The spread wedge instead captures the nonlinearities that arise when short term rates are close to the lower bound. This means that the spread wedge measures by how much the lower bound is distorting the observed sovereign spread with respect to the shadow one. Its size depends on the distance of the forward curves of the two countries from the lower bound, and also on the volatilities of their future shadow short term rates under the risk-neutral probability measure. As the forward curve of one of the two countries approaches the lower bound, and/or the volatility of its future shadow rates increases, a larger proportion of the observed spread is determined by the spread wedge and, as a consequence, the observed spread looses its informational content as a measure of sovereign risk.

We estimate our joint shadow rate term structure model by quasi-maximum likelihood and the Extended Kalman filter using zero rates computed from Euro area overnight index swaps (OIS), and German and Italian Treasury yields for the period January 2001 to October 2016. Following other recent work on the subject, we use OIS rates as a proxy for risk-free rates in the Euro area; therefore, the spread of one country's yield with respect to the same maturity OIS one can be interpreted as a measure of its sovereign risk or safety premium. We specify a model with four factors: two common to the three curves, one specific to Germany and another one specific to Italy.

Our results show that spread wedges became non-negligible since 2012, indicating the presence of strong nonlinearities in the behavior of long term sovereign spreads at the interest rate lower bound. In particular, we find that the 10-year Italian shadow sovereign spread with respect to the OIS rate was larger than the corresponding observed spread. This indicates that, in this period, the interest rate lower bound was constraining OIS rates more than the Italian ones, and that in the absence of a lower bound the 10-year Italian spread with respect to the OIS rate would have been larger. On the contrary, the 10-year German shadow sovereign spread with respect to the OIS rate was lower than the observed spread. This indicates that, in the lower bound period, German rates were more constrained than the OIS ones, and that in the absence of a lower bound the 10-year German spread with respect to the OIS rate would have been lower. We also find that, in the absence of a lower bound, in 2012 the 10-year Italian spread with respect to Germany would have been higher by as much as 77 basis points.

Our focus on the behaviour of sovereign spreads when interest rates are at or near the lower bound is novel and allows to highlight three important implications. First, as interest rates approach their lower bound, the conditional distribution of future spreads becomes skewed. For the case of the spreads between Italian and German yields, we find that the distribution of future spreads is skewed to the right and that the degree of skewness decreases with the maturity, but is still substantial even for the spread between 10 year yields at a 1 year horizon. Second, spreads depend on the distance from the lower bound. This implies that an exogenous change in the lower bound affects the observed spread even if the sovereign risk does not change. More specifically, our results indicate that an exogenous decrease of the lower bound by 20 basis points increases the 10-year spread between Italian and German yields by as much as 8 basis points. Third, at or near the interest rate lower bound, the observed spread looses its informational content as a measure of sovereign risk but the shadow spread does not. In particular, we find that the relation between the 10 year sovereign Credit Default Swaps (CDS) spread of Italy with respect to Germany and the observed 10 year sovereign spread between Italian and German yields broke down because of a structural break around the end 2011/beginning 2012, when the German forward curve became close to the lower bound. On the contrary, the relation between the 10 year sovereign CDS spread and the 10-year sovereign shadow spread remained stable over the entire sample.

This paper also contributes to the literature on shadow rate term structure models by considering a multi-country framework and by providing evidence supporting the conjecture that the lower bound on Euro area rates is not constant over time. Multi-country affine term structure models have been classified by Egorov, Li and Ng (2011), and are extensively used to investigate the interactions between domestic and foreign yield curves. However, the literature on shadow rate term structure models focuses exclusively on domestic settings, mainly because shadow rate models are computationally more intensive than standard affine ones. In addition, the identification restrictions used by Wu and Xia (2016) and Krippner (2012) do not naturally extend to a multiple yield curve setup, as they require the researcher to specify the nature of the latent states, in addition to their number. Carriero, Mouabbi and Vangelista (2016) estimate a joint shadow rate model on nominal and inflation indexed UK interest rates, imposing the lower bound constraint only on the nominal yield curve.

Dawachter, Iania and Wijnandts (2016) use a similar framework to model risk-free rates and sovereign spreads. To the best of our knowledge, our paper is the first study of a multi-country shadow rate term structure model.

Usually, shadow rate term structure models assume that the lower bound is constant over time; its value is either fixed a priori, calibrated or estimated. This assumption seems appropriate for Japanese yields (see Ichiue, Ueno et al. 2007, Kim and Singleton 2012), US yields (see Krippner 2012, Kim and Priebsch 2013, Christensen and Rudebusch 2016, Bauer and Rudebusch 2016, Wu and Xia 2016), and UK yields (see Andreasen and Meldrum 2015). However, the assumption of a constant lower bound is rejected for Euro area yields by Lemke and Vladu (2017). Kortela (2016) and Wu and Xia (2017) find that a time-varying lower bound is better suited for European yields. Accordingly, in this paper, we assume that the lower bound depends on the short term risk-free rate for reserves at the European Central Bank (ECB) and on some unknown parameters to be estimated.

The paper is organized as follows. Section 2 describes the joint shadow rate term structure model and how to derive sovereign shadow spreads. Section 3 describes the data and performs some preliminary analysis. Section 4 describes the estimation methodology and the identification scheme. Section 5 describes the results and, finally, Section 6 concludes.

2 A joint shadow rate term structure model for yield curves in a monetary union

2.1 Setup

We model the joint dynamics of the risk-free, the German and the Italian yield curves using a nonlinear model with common and country-specific latent factors evolving according to linear Gaussian dynamics. Shadow interest rates are affine in the state variables, but observed rates are bounded by a time-varying exogenous lower bound. In this section, we describe each point in detail.

We assume that the *shadow* risk-free short term interest rate s_t^0 is an affine function of n_0 common factors $\boldsymbol{x}_t^0$ related to the common monetary policy. We also assume that the German and the Italian *shadow* short term interest rates, s_t^i, $i = GE, IT$, are affine function of both the common factors $\boldsymbol{x}_t^0$ and of n_i country-specific factors $\boldsymbol{x}_t^i$, driven by credit quality or liquidity. Let $n = n_0 + n_{GE} + n_{IT}$, and denote the full $n \times 1$ vector of state variables as

$$\boldsymbol{x}_t = (\boldsymbol{x}_t^{0\prime}, \boldsymbol{x}_t^{GE\prime}, \boldsymbol{x}_t^{IT\prime})'.$$

Shadow rates can then be expressed as[1]

$$s_t^i = \delta_0^i + \boldsymbol{\delta}_1^{i\prime} \boldsymbol{x}_t, \quad i = 0, GE, IT, \tag{1}$$

where:[2]

$$\boldsymbol{\delta}_1^0 = \begin{pmatrix} \boldsymbol{\delta}_1^{0,0} \\ \mathbf{0}_{n_{GE}\times 1} \\ \mathbf{0}_{n_{IT}\times 1} \end{pmatrix}, \quad \boldsymbol{\delta}_1^{GE} = \begin{pmatrix} \boldsymbol{\delta}_1^{GE,0} \\ \boldsymbol{\delta}_1^{GE,GE} \\ \mathbf{0}_{n_{IT}\times 1} \end{pmatrix}, \quad \boldsymbol{\delta}_1^{IT} = \begin{pmatrix} \boldsymbol{\delta}_1^{IT,0} \\ \mathbf{0}_{n_{GE}\times 1} \\ \boldsymbol{\delta}_1^{IT,IT} \end{pmatrix}.$$

We assume that the state variables follow a first order vector autoregressive process under the physical measure $\mathbb{P}$

$$\boldsymbol{x}_{t+1} = \boldsymbol{\mu} + \boldsymbol{\Phi} \boldsymbol{x}_t + \boldsymbol{\Gamma} \boldsymbol{\varepsilon}_{t+1}, \tag{2}$$

where $\boldsymbol{\varepsilon}_{t+1} \overset{\mathbb{P}}{\sim} \mathcal{N}_{IID}(\mathbf{0}, \mathbf{I}_n)$ and $\boldsymbol{\Gamma}$ is a lower triangular matrix. We also assume that there exists a risk-neutral probability measure $\mathbb{Q}$ which prices all financial assets and under which the risk factors follow a first order Gaussian vector autoregression

$$\boldsymbol{x}_{t+1} = \boldsymbol{\mu}^{\mathbb{Q}} + \boldsymbol{\Phi}^{\mathbb{Q}} \boldsymbol{x}_t + \boldsymbol{\Gamma} \boldsymbol{\varepsilon}_{t+1}^{\mathbb{Q}}, \tag{3}$$

where $\boldsymbol{\varepsilon}_{t+1}^{\mathbb{Q}} \overset{\mathbb{Q}}{\sim} \mathcal{N}_{IID}(\mathbf{0}, \mathbf{I}_n)$. To ensure that $\boldsymbol{x}_t^{GE}$ and $\boldsymbol{x}_t^{IT}$ are country-specific factors, we impose that the $(n_{GE} + n_{IT}) \times (n_{GE} + n_{IT})$ lower right block of $\boldsymbol{\Phi}^{\mathbb{Q}}$ is block-diagonal.

Under the no-arbitrage condition, the price $p_{t,\tau}^i$ of a zero-coupon bond with τ months to

[1] In what follows, we refer to the risk-free yield curve as the yield curve of country 0.

[2] In contingent claims valuation models in the presence of default or liquidity risk (see Duffie and Singleton 1997, 1999), the shadow short rate for Italy could be interpreted as the default-adjusted shadow short-rate, where a single country-specific factor x_t^{IT} would be given by the product of the hazard rate for default at time t and the expected fractional loss in market value if default were to occur at time t. In the same way, the shadow short rate for Germany could be interpreted as a liquidity-adjusted shadow short rate, where x_t^{GE} would represent the convenience yield of holding German bonds.

maturity in country i can be expressed as

$$p_{t,\tau}^{i} = E_t^{\mathbb{Q}}\left[\exp\left(-\sum_{j=0}^{\tau-1} r_{t+j}^{i}\right)\right], \quad i = 0, GE, IT$$

where r_t^i is the short term interest rate in country i. In the Gaussian affine term structure model, the short term interest rate is equal to the shadow short rate defined in (1), i.e. $r_t^i = s_t^i$. Under this assumption, bond prices $p_{t,\tau}^i$ are exponentially affine in the state variables $\boldsymbol{x}_t$, which implies that the corresponding yields $y_{t,\tau}^i = -\log(p_{t,\tau}^i)/\tau$ are affine in $\boldsymbol{x}_t$. This model has been extensively used to model term structures of interest rates (see Piazzesi 2010). However, due to the fact that the Gaussian affine term structure model does not bound interest rates, it cannot account for the near-lower bound behavior of the yield curve: it can neither prevent interest rates from decreasing below the bound, nor replicate short rates that stay close to the lower bound for a prolonged period of time.

The lower bound on interest rates can be enforced by allowing the short term interest rate to be equal to the shadow short rate only when the latter is above the lower bound, and otherwise equal to the lower bound:

$$r_t^i = \max(s_t^i, \underline{r}_t), \quad i = 0, GE, IT. \tag{4}$$

This is the shadow rate term structure model firstly introduced by Black (1995). The idea is that short term interest rates are bounded below due to the option to convert to currency. As a result of this currency option, all term rates are bounded but do not have a reflecting boundary condition, as opposed to affine models with factors that follow square-root processes or quadratic Gaussian models. An appealing feature of the shadow rate term structure model is that, when short term interest rates are far from the lower bound, interest rates behave as in a Gaussian affine term structure model. Notice that $\underline{r}_t$ can be slightly positive, zero or negative as it represents the return of holding Euros (net of the costs associated with storing, insuring and transferring large amounts of currency), which is common across the three yield curves.

2.2 Solution

The assumption in (4) implies that yields are nonlinear in state variables and do not have an analytical expression. Denote by $f^i_{t,\tau}$ the time t one period forward rate in country i for a loan starting at $t+\tau$. Forward rates and bond yields are related by the following general property:

$$y^i_{t,\tau} = \frac{1}{\tau}\sum_{j=0}^{\tau-1} f^i_{t,j}, \quad i = 0, GE, IT. \tag{5}$$

Wu and Xia (2016) show that, under (1), (3) and (4), the forward rate $f^i_{t,\tau}$ is approximately equal to

$$f^i_{t,\tau} \approx \underline{r}_t + \sigma^i_\tau g\left(\frac{a^i_\tau + \boldsymbol{b}^{i\prime}_\tau \boldsymbol{x}_t - \underline{r}_t}{\sigma^i_\tau}\right), \quad i = 0, GE, IT, \tag{6}$$

where:

$$\begin{aligned}
g(z) &= zN(z) + n(z),\\
\boldsymbol{b}^i_\tau &= \left[(\boldsymbol{\Phi}^{\mathbb{Q}})^\tau\right]' \boldsymbol{\delta}^i_1,\\
a^i_\tau &= \delta^i_0 + \left(\sum_{j=0}^{\tau-1}\boldsymbol{b}^i_j\right)' \boldsymbol{\mu}^{\mathbb{Q}} - \frac{1}{2}\left(\sum_{j=0}^{\tau-1}\boldsymbol{b}^i_j\right)' \boldsymbol{\Gamma}\boldsymbol{\Gamma}' \left(\sum_{j=0}^{\tau-1}\boldsymbol{b}^i_j\right),\\
\left(\sigma^i_\tau\right)^2 &= \sum_{j=0}^{\tau-1} \boldsymbol{b}^{i\prime}_j \boldsymbol{\Gamma}\boldsymbol{\Gamma}' \boldsymbol{b}^i_j,
\end{aligned} \tag{7}$$

with $N(\cdot)$ and $n(\cdot)$ denoting the cdf and the pdf of the standard normal distribution, respectively. The approximation in (6) only holds for $\tau \geq 1$. For $\tau = 0$, given $f^i_{t,0} = r^i_t$, (4) implies

$$f^i_{t,0} = \underline{r}_t + \max(0, \delta^i_0 + \boldsymbol{\delta}^{i\prime}_1 \boldsymbol{x}_t - \underline{r}_t), \quad i = 0, GE, IT. \tag{8}$$

Plugging the approximate expressions for the forward rates in (6) and (8) into (5), we can construct an approximation for the yields $y^i_{t,\tau}$:

$$y^i_{t,\tau} = \underline{r}_t + \frac{1}{\tau}\left[\max(0, \delta^i_0 + \boldsymbol{\delta}^{i\prime}_1 \boldsymbol{x}_t - \underline{r}_t) + \sum_{j=1}^{\tau-1} \sigma^i_j g\left(\frac{a^i_j + \boldsymbol{b}^{i\prime}_j \boldsymbol{x}_t - \underline{r}_t}{\sigma^i_j}\right)\right] = h^i_\tau(\boldsymbol{x}_t) \tag{9}$$

for $i = 0, GE, IT$.

2.3 Shadow yield curve

The short rate equation (4) introduces nonlinearity into a term structure model with linear Gaussian dynamics and, as a consequence, yields are nonlinear in the state variables. The model however allows to compute shadow yields, i.e. the interest rates that we would observe in the absence of the lower bound. The latter does not restrict shadow rates, which are thus always linear in the state variables.

The short rate equation (4) can be written as

$$r_t^i = f_{t,0}^i = s_t^i + \max(\underline{r}_t - s_t^i, 0), \quad i = 0, GE, IT, \tag{10}$$

where s_t^i is linear in the state variables, see (1), and $\max(\underline{r}_t - s_t^i, 0)$ represents the option value of cash, see Krippner (2015). A similar decomposition for forward rates with $\tau \geq 1$ can be derived using the approximation in (6). In particular, if we define shadow forward rates $\tilde{f}_{t,\tau}^i$ as

$$\tilde{f}_{t,\tau}^i = a_\tau^i + \boldsymbol{b}_\tau^{i\prime} \boldsymbol{x}_t, , \quad i = 0, GE, IT \tag{11}$$

we can rewrite (6) as:

$$f_{t,\tau}^i = \tilde{f}_{t,\tau}^i + z_{t,\tau}^i, \quad i = 0, GE, IT, \tag{12}$$

where the option value of cash $z_{t,\tau}^i$ is given by

$$z_{t,\tau}^i = \left(\underline{r}_t - \tilde{f}_{t,\tau}^i\right) \left[1 - N\left(\frac{\tilde{f}_{t,\tau}^i - \underline{r}_t}{\sigma_\tau^i}\right)\right] + \sigma_\tau^i \, n\left(\frac{\tilde{f}_{t,\tau}^i - \underline{r}_t}{\sigma_\tau^i}\right) > 0, \quad i = 0, GE, IT. \tag{13}$$

As shown in the top plot in figure 1, the option value of cash $z_{t,\tau}^i$ depends on both the distance of the shadow forward rate from the lower bound $(\tilde{f}_{t,\tau}^i - \underline{r}_t)$ and on the conditional volatility of the τ-periods ahead shadow short rate of country i under the risk-neutral distribution, σ_τ^i defined in (7). The option value of cash is large and positive when shadow forward rates are close or below the lower bound, otherwise it is negligible. In addition, the larger the future shadow rate volatility under the risk-neutral measure, the larger the option value of cash.

Given that the option value of cash is always greater than zero, equation (12) implies that the observed forward rate is always greater than the corresponding shadow forward rate, i.e. $f_{t,\tau}^i \geq \tilde{f}_{t,\tau}^i$. The difference between the two is larger (i) the closer the observed short term

Figure 1: Option value of cash and lower bound wedge

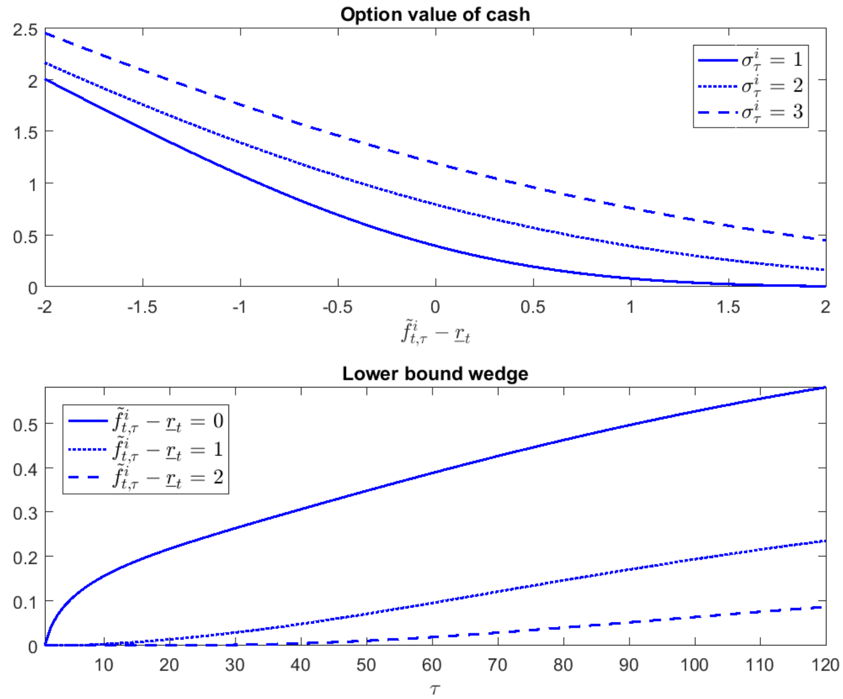

The top figure plots the option value of cash $z^i_{t,\tau}$ defined in (13) as a function of the distance of the shadow forward rate from the lower bound $\tilde{f}^i_{t,\tau} - \underline{r}_t$ and for different values of the future shadow rate volatility under the risk-neutral measure σ^i_τ. The bottom figure illustrates the lower bound wedge $Z^i_{t,\tau}$ defined in (17) as a function of the maturity τ and for different values of the distance of the shadow forward rate from the lower bound $\tilde{f}^i_{t,\tau} - \underline{r}_t$. The lower bound wedges are computed assuming a flat forward curve, and a curve for the future shadow rate volatility that matches the curve estimated on OIS rates, reported in figure 8. All values are in percentage points.

rate is to the lower bound and (ii) the larger the volatility of future shadow short rates. The reason for (i) is that close to the lower bound, agents understand that the range of possible realizations of future short term interest rates is larger above than below the current level, and therefore the distribution of future rates is skewed to the right, which in turn implies $f^i_{t,\tau} = E^{\mathbb{Q}}(r_{t+\tau}|\boldsymbol{x}_t) > E^{\mathbb{Q}}(s_{t+\tau}|\boldsymbol{x}_t) = \tilde{f}^i_{t,\tau}$. The reason for (ii) is that the larger the conditional volatility of future shadow short rates, the more likely it is that the range of possible values of future shadow short rates includes values that are below the lower bound. This again implies a large difference between expected future short rates and expected future shadow rates (under the $\mathbb{Q}$ distribution), and a larger option value of cash.

The option value of cash generates a wedge between observed and shadow yields at any maturity. To see this, substitute the decompositions (10) and (12) in (5), to obtain:

$$y^i_{t,\tau} = \tilde{y}^i_{t,\tau} + Z^i_{t,\tau}, \quad i = 0, GE, IT, \tag{14}$$

where the shadow yield $\tilde{y}^i_{t,\tau}$ is given by

$$\tilde{y}^i_{t,\tau} = \frac{1}{\tau}\sum_{j=0}^{\tau-1}\tilde{f}^i_{t,\tau} = \frac{1}{\tau}\left[\delta^i_0 + \boldsymbol{\delta}^{i\prime}_1\boldsymbol{x}_t + \sum_{j=1}^{\tau-1}\left(a^i_j + \boldsymbol{b}^{i\prime}_j\boldsymbol{x}_t\right)\right] = A^i_\tau + \mathbf{B}^{i\prime}_\tau\boldsymbol{x}_t, \quad i = 0, GE, IT, \tag{15}$$

with

$$A^i_\tau = \frac{1}{\tau}\left(\delta^i_0 + \sum_{j=1}^{\tau-1}a^i_j\right), \quad \mathbf{B}^i_\tau = \frac{1}{\tau}\left(\boldsymbol{\delta}^i_1 + \sum_{j=1}^{\tau-1}\boldsymbol{b}^i_j\right), \quad i = 0, GE, IT, \tag{16}$$

and the lower bound wedge $Z^i_{t,\tau}$ is given by

$$Z^i_{t,\tau} = \frac{1}{\tau}\left[\max(\underline{r}_t - s^i_t, 0) + \sum_{j=1}^{\tau-1}z^i_{t,j}\right] > 0, \quad i = 0, GE, IT. \tag{17}$$

Equation (14) shows that shadow rate term structure models allow to decompose observed yields in two components: the shadow yield $\tilde{y}^i_{t,\tau}$ (which is linear in the state variables) and the lower bound wedge $Z^i_{t,\tau}$ (which is the cumulative sum of the option values of cash). Thus, observed yields are always greater than the corresponding shadow yields, i.e. $y^i_{t,\tau} \geq \tilde{y}^i_{t,\tau}$. The difference among the two is the lower bound wedge generated by the nonlinearities that arise at the lower bound and that can be seen as a measure of how tightly the lower bound constrains the observed yield, see Krippner (2015) and Bauer and Rudebusch (2016). As yields move away from the lower bound, the wedge becomes negligible and observed yields approach their shadow counterparts.

The bottom plot of Figure 1 reports the lower bound wedge as a function of the maturity of the bond, for different values of the distance of the shadow forward rate from the lower bound and for a flat forward curve. As expected, the lower bound wedge is larger when the shadow forward rate is closer to the lower bound. Notice that the lower bound wedge increases with the maturity of the yields because the option value of cash is always positive.

2.4 Sovereign spreads at the interest rate lower bound

Sovereign spreads measure sovereign risk premia and are directly related to sovereign risk. We define the sovereign spread between yields of countries i and j with maturity τ as

$$\Delta^{i,j}_{t,\tau} = y^i_{t,\tau} - y^j_{t,\tau}, \quad i, j = 0, GE, IT.$$

In our no-arbitrage framework, long term sovereign spreads are determined by current and expected short term sovereign spreads (under the risk-neutral distribution). Therefore as short term interest rates approach their lower bound, short term current and expected spreads are constrained by it and, as a consequence, the long term spreads as well.

In order to assess the effect of the interest rate lower bound on sovereign spreads, we use (14) to decompose observed sovereign spreads as

$$\Delta^{i,j}_{t,\tau} = \tilde{\Delta}^{i,j}_{t,\tau} + Z^{i,j}_{t,\tau}, \quad i, j = 0, GE, IT, \tag{18}$$

where the shadow sovereign spread $\tilde{\Delta}^{i,j}_{t,\tau}$ is given by

$$\tilde{\Delta}^{i,j}_{t,\tau} = \tilde{y}^i_{t,\tau} - \tilde{y}^j_{t,\tau}, \tag{19}$$

and the sovereign spread wedge $Z^{i,j}_{t,\tau}$ is

$$Z^{i,j}_{t,\tau} = Z^i_{t,\tau} - Z^j_{t,\tau} = \frac{1}{\tau}\left[\max(\underline{r}_t - s^i_t, 0) - \max(\underline{r}_t - s^j_t, 0) + \sum_{s=1}^{\tau-1}(z^i_{t,s} - z^j_{t,s})\right]. \tag{20}$$

Equation (18) shows that the observed sovereign spread can be decomposed in two components: the shadow spread $\tilde{\Delta}^{i,j}_{t,\tau}$ that we would observe if rates in the two countries were far from the lower bound, and the sovereign spread wedge $Z^{ij}_{t,\tau}$, that measures the nonlinearities that arise at the lower bound, i.e. by how much the lower bound is distorting the observed sovereign spread with respect to the shadow spread. The latter depends on the distance of each of the two forward curves from the lower bound and on the volatilities under $\mathbb{Q}$ of future shadow rates in each country.

The sovereign spread wedge is the difference between expected future short term spreads and shadow spreads, both under $\mathbb{Q}$. If for one country the short term rate approaches the lower bound, or the conditional volatilities of future shadow short rates increases, agents understand that the range of possible values of its future short term interest rates is larger above than below the current short term rate. This implies that expected future short term spreads are above (if the constrained country is i) or below (if the constrained country is j) the current short term spread.

Let us assume for simplicity that the conditional volatilities of the first τ-periods ahead shadow short rates under the risk-neutral distribution are the same for both countries. In this case, if the forward rates of the two countries are far from the lower bound, the sovereign spread wedge is negligible and the observed spread is close to the shadow spread. However, if at least one of the two forward curves is close to the lower bound, the sovereign spread wedge is non-negligible and the observed spread is different from the shadow spread. The sign of the sovereign spread wedge depends on which of the two forward curves is closer to the lower bound, and thus more constrained by it.

To further simplify the discussion, let us consider $\Delta^{i,0}_{t,\tau}$, i.e. the spread of country i's yield with maturity τ with respect to the risk-free yield with the same maturity. In the presence of a positive sovereign risk, the yield curve of country i is above the risk-free yield curve and, as rates decline towards the lower bound, the risk-free yield curve becomes more constrained by it, i.e. $Z^0_{t,\tau} \geq Z^i_{t,\tau}$. This implies that the sovereign spread wedge is negative, i.e. $Z^{i0}_{t,\tau} \leq 0$, and the observed spread is smaller than the shadow spread, i.e. $0 \leq \Delta^i_{t,\tau} \leq \tilde{\Delta}^i_{t,\tau}$. The opposite happens in the presence of a negative sovereign risk, i.e. flight to safety, as in this case the yield curve of country i is below the risk-free yield curve and, as rates decrease towards the lower bound, the yield curve of country i becomes more constrained by the bound than the risk-free yield curve, i.e $Z^i_{t,\tau} \geq Z^0_{t,\tau}$. This implies that the sovereign spread wedge is greater than zero, i.e $Z^{i0}_{t,\tau} \geq 0$, and the observed spread is larger than the shadow spread, i.e. $\tilde{\Delta}^i_{t,\tau} \leq \Delta^i_{t,\tau} \leq 0$.

The upshot of Equation (18) is that, as short term rates approach the lower bound, the observed spread looses its informational content as a measure of sovereign risk. A decrease in the observed spread could be either due to a decrease of the shadow spread or to a decrease of the sovereign spread wedge. However, while changes in the shadow spread are solely determined by sovereign risk, changes in the sovereign spread wedge also depend on the distance of the two yield curves from the lower bound. For example, in the presence of sovereign risk, an exogenous decrease of the lower bound decreases the wedge on risk-free rates more than on rates of country i, and thus increases the sovereign spread wedge. This implies that also the observed spread increases, even if the shadow spread and the sovereign risk are not affected. For this reason, when interest rates are constrained by the lower bound, the shadow spread is a more informative measure of the sovereign risk.

3 Data and preliminary evidence

We use end-of-month zero-coupon rates on German and Italian Treasury bonds, and on OIS based on EONIA (the overnight unsecured interbank rate in the Euro Area). All data are provided by Datastream-Eikon and span the period January 2001 to October 2016 for maturities 6 months, 1, 2, 3, 5, 7 and 10 years.

As in recent studies on Euro Area yield curves, see Lemke and Vladu (2017), Pericoli and Taboga (2015) and Kortela (2016), we use OIS rates to proxy for risk-free rates in the Euro Area. This because the OIS market is liquid for all maturities, and the credit risk of overnight deposits is very small. We convert the OIS rates provided by Datastream-Eikon to zero-coupon rates using a bootstrapping method. OIS rates with maturity 3 years are available from December 2004, and OIS rates with longer maturities are available from August 2005. German and Italian zero-coupon rates with maturity 6 months are not available before 2007; for this maturity we use the zero-coupon rates provided by the Deutsche Bundesbank and the Italian Ministry of Economy and Finance up to December 2006.

To model the lower bound, we use the deposit facility rate of the Eurosystem. This is a monetary policy instrument under the direct control of the ECB, as it is the short term risk-free rate for reserves at Euro area banks. End of month data for the Euro overnight interest rate is obtained from Datastream. In the last section of the paper, we relate spreads and shadow spreads to sovereign credit default swap (CDS) spreads. To this end we use end of month data on 10-year Italian and German CDS spreads from Datastream. The first observation available for both CDS spreads is December 2007.

In figure 2 we plot the full dataset of yields used in the analysis. Risk-free, German and Italian rates started with similar values at the beginning of the sample but began to diverge in 2009. Italian rates started to increase in 2010 and spiked at the end of 2011, due to an increase in the sovereign risk premium. On the contrary, risk-free and German rates steadily decreased towards zero. Risk-free short rates reached zero by mid-2012, but due to a flight to quality in the European bond market, also driven by the fact that German bonds are heavily used as collateral for short term borrowing in repo markets, German short rates reached zero already at the end of 2011. Risk-free and German short rates stayed at

Figure 2: Data

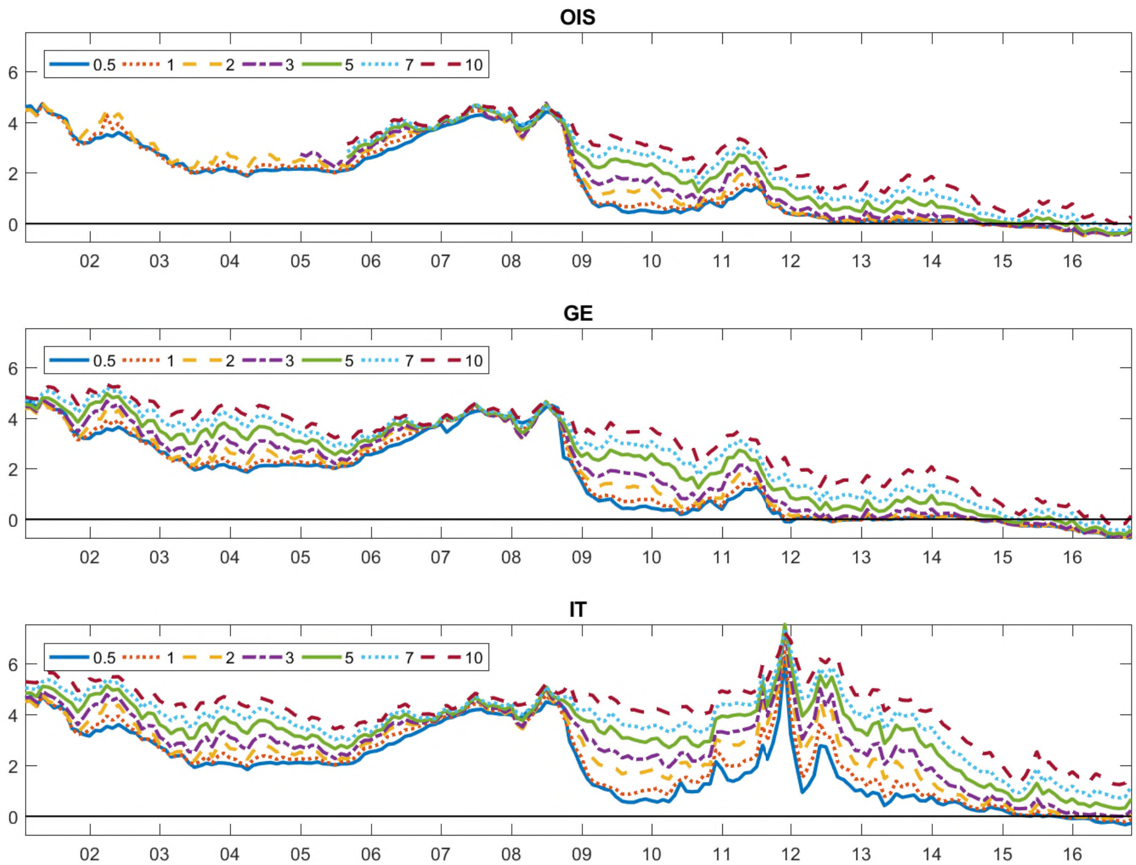

This figure reports end-of-month zero-coupon rates on OIS based on EONIA (top plot), German Treasury bonds (middle plot) and Italian Treasury bonds (bottom plot). The sample is January 2001 to October 2016 and the maturities are 6 months, 1, 2, 3, 5, 7 and 10 years. OIS rates with maturity 3 years are available from December 2004, and OIS rates with longer maturities are available from August 2005.

zero until mid-2014, when they turned negative. Italian short rates reached zero only at the beginning of 2015 and became negative at the end of the year. Figure 2 also shows that the whole German yield curve and almost the entire risk-free yield curve (with the exception of the 10 year rate) are negative in the last part of 2016. In this period, the long-short rate spread for risk-free and German rates is much lower than the Italian one.

Figure 3: Yields and ECB deposit rate

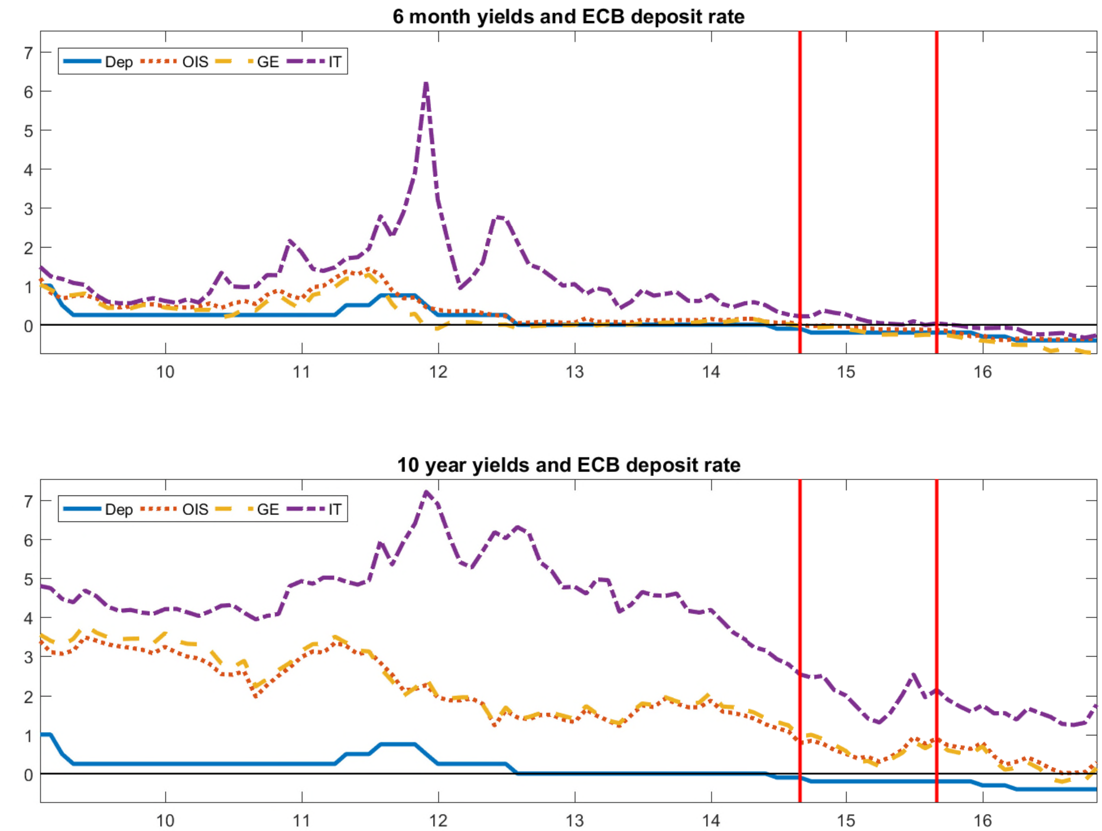

This figure reports the ECB deposit rate along with OIS, German and Italian yields with maturity 6 months (top plot) and 10 years (bottom plot). The red vertical lines denote August 2014 and August 2015.

3.1 Lower bound specification

The behaviour of yields in figure 2 highlights the need for a time-varying lower bound specification, as also noted by Lemke and Vladu (2017), Kortela (2016) and Wu and Xia (2017). To investigate the behaviour of the lower bound, in figure 3 we plot the 6 month and the 10 year risk-free, German and Italian yields along with the deposit facility rate of the Eurosystem.

Figure 3 shows that the 10 year rates are always above the ECB deposit rate. For the 6 months rates, however, we can identify three subperiods. The first is up to August 2014, in which short term rates are bounded from below either by zero or the deposit rate.[3] The

[3]Lemke and Vladu (2017) find a significant change in the lower bound parameter in August 2014.

second is from September 2014 to August 2015, when risk-free and German rates turned negative. The last subperiod is from October 2015 to the end of the sample, when short term risk-free and German rates are negative and below the ECB deposit rate. These three subperiods are highlighted with red vertical lines in figure 3. Accordingly, we model the lower bound as follows:

$$\underline{r}_t = \min(0, d_t) + \theta_t, \tag{21}$$

where d_t is the ECB deposit rate and θ_t is defined as

$$\theta_t = \begin{cases} \theta_1, & t \leq \text{August 2014} \\ \theta_2, & \text{August 2014} < t \leq \text{August 2015} \\ \theta_3, & t > \text{August 2015}. \end{cases} \tag{22}$$

This specification for the lower bound implies that if $\theta_t = 0$ and $d_t \geq 0$, short term interest rates are bounded by zero due to the option to convert to currency. If instead $\theta_t = 0$ and $d_t < 0$, short term interest rates are bounded by the deposit rate, as banks do not lend at a rate lower than the one they could get on overnight deposits with the central bank. However, if $\theta_t \neq 0$, the effective lower bound is different than the floor for interest rates given by either zero or the deposit rate. As noted by Lemke and Vladu (2017), the effective lower bound is the bound perceived by market participants and a $\theta_t \neq 0$ allows it to be different from zero or the deposit rate. The parameters θ_1, θ_2 and θ_3 will be estimated along with the other model parameters.

We assume that, when pricing bonds and swaps, agents expect the same lower bound to prevail for the future (see the discussion in Lemke and Vladu 2017, Kortela 2016), even if they are aware of the possibility that the bound parameter may change.

3.2 Model specification

The joint shadow rate term structure model in section 2 allows the risk-free and the country yield curves to be driven by common and country-specific factors. To determine the number of each type of factors, we perform a principal component analysis. We start by analyzing each yield curve separately. The first three columns of Table 1 report the cumulative variance of risk-free, German and Italian zero-coupon yields explained by the corresponding first six principal components (PCs) extracted separately for each country. The table indicates for

Table 1: Cumulative variance explained by principal components

	Risk-free	Germany	Italy	Joint
PC1	0.969	0.958	0.908	0.830
PC2	0.999	0.998	0.997	0.963
PC3	1.000	1.000	0.999	0.994
PC4	1.000	1.000	1.000	0.998
PC5	1.000	1.000	1.000	0.999
PC6	1.000	1.000	1.000	0.999

Note: this table reports the cumulative percentage of variance of risk-free yields (first column), German yields (second column), Italian yields (third column) and joint (fourth column) explained by the first six PCs extracted from risk-free yields (first column), German yields (second column), Italian yields (third column), and jointly from risk-free, German and Italian yields (fourth column).

all three term structures the first two PCs explain a large fraction of the observed variance (99.9% for OIS, 99.8% for Germany and 99.7% for Italy).

We then pool the three yield curves and extract PCs jointly. The cumulative joint variance of risk-free, German and Italian yields explained by these joint PCs is reported in the last column of Table 1. The table shows that four joint PCs are required to explain at least 99.8% of the joint variation in risk-free, German and Italian yields. This indicates that the German and the Italian yield curves are driven by country-specific factors, in addition to common factors.

Given that the risk-free yield curve is driven only by the common risk-free factors, the PCs extracted from the risk-free yield curve proxy for the common risk-free factors. To assess the relation of the common risk-free factors with the country factors, we analyze how much of the variation in the first three country PCs is explained by the risk-free factors. In Table 2, we report the R^2 from regressing German and Italian PCs on the risk-free PCs. The table indicates that the first German PC is perfectly explained by the first risk-free PC, and that the second German PC is mostly explained by the second risk-free PC. The PCs extracted from Italian yields are less related to the risk-free PCs, and even using all six risk-free PCs we can only explain up to 71% and 82% of the first and second Italian PC, indicating that Italian yields are driven by a strong country-specific component.

Table 2: Common Factors

# Common PC	Germany PC1	Germany PC2	Germany PC3	Italy PC1	Italy PC2	Italy PC3
1	0.996	0.001	0.000	0.522	0.228	0.005
First 2	0.997	0.967	0.000	0.559	0.736	0.007
First 3	0.998	0.968	0.713	0.663	0.775	0.364
First 4	0.998	0.968	0.810	0.680	0.818	0.368
First 5	0.998	0.968	0.818	0.711	0.818	0.422
First 6	0.998	0.969	0.818	0.711	0.818	0.423

Note: this table reports the R^2 from regressing German and Italian PCs on the risk-free PCs. The first row refers to regressions on the first risk-free PC, the second row refers to regressions on the first two risk-free PCs, and so on.

To assess the number of country-specific factors, we extract country PCs from the residuals of the regression of German and Italian yields on the first one or two risk-free PCs. In Table 3, we report the percentage of variance of German and Italian residuals explained by the first six country PCs. For comparison, in the first and the fourth column we report the explained variance of German and Italian yields when no common components are extracted (this replicates the information reported in Table 1). The table indicates that, after taking into account the two common factors, Italian yields are driven by one country factor. For the German yields, the evidence for country-specific factors is less clear. However, as reported in Table 2, the two risk-free PCs explain 96.7% of the variation of the German PCs, and only 73.6% of the variation of the Italian PCs.

Overall, Tables 1-3 suggest that four factors are needed to explain the three yield curves; two of these factors are the common risk-free factors and the other two are specific to each country. Accordingly, in specifying our model we choose $n = 4$, $n_0 = 2$, $n_{GE} = n_{IT} = 1$.

4 Inference

4.1 Estimation

We estimate the joint shadow rate term structure model by quasi maximum likelihood using a state space representation. The sample consists of panels for $y^0_{t,\tau}$, $y^{GE}_{t,\tau}$ and $y^{IT}_{t,\tau}$, $t = 1, \dots, T$

Table 3: Country Factors

	Germany			Italy		
# Common PC	0	1	2	0	1	2
1 Country PC	0.958	0.726	0.485	0.908	0.878	0.953
2 Country PC	0.040	0.181	0.260	0.089	0.115	0.040
3 Country PC	0.002	0.084	0.211	0.002	0.005	0.005
4 Country PC	0.000	0.006	0.034	0.001	0.001	0.001
5 Country PC	0.000	0.002	0.007	0.000	0.000	0.000
6 Country PC	0.000	0.001	0.003	0.000	0.000	0.000

Note: this table reports the percentage of variance of German and Italian yield residuals explained by the first 6 country PCs. The first and the fourth column refer to the percentage of variance of German and Italian yields. The second and fifth column refer to the percentage of variance of the residuals of German and Italian yields after they are regressed on the first common factor. The third and the sixth refer to the percentage of variance of the residuals of German and Italian yields after they are regressed on the first two common factors.

and $\tau = \tau_1, \ldots, \tau_K$. Let us denote the observed yields by:

$$\boldsymbol{y}_t = (\boldsymbol{y}_t^{0\prime}, \boldsymbol{y}_t^{GE\prime}, \boldsymbol{y}_t^{IT\prime})',$$

with $\boldsymbol{y}_t^0 = (y_{t,\tau_1}^0, \ldots, y_{t,\tau_K}^0)'$, $\boldsymbol{y}_t^{GE} = (y_{t,\tau_1}^{GE}, \ldots, y_{t,\tau_K}^{GE})'$ and $\boldsymbol{y}_t^{IT} = (y_{t,\tau_1}^{IT}, \ldots, y_{t,\tau_K}^{IT})'$, and the model implied yields by:

$$\boldsymbol{h}(\boldsymbol{x}_t) = [\boldsymbol{h}^0(\boldsymbol{x}_t)', \boldsymbol{h}^{GE}(\boldsymbol{x}_t)', \boldsymbol{h}^{IT}(\boldsymbol{x}_t)']',$$

with $\boldsymbol{h}^0(\boldsymbol{x}_t) = [h_1^0(\boldsymbol{x}_t), \ldots, h_K^0(\boldsymbol{x}_t]'$, $\boldsymbol{h}^{GE}(\boldsymbol{x}_t) = [h_1^{GE}(\boldsymbol{x}_t), \ldots, h_K^{GE}(\boldsymbol{x}_t]'$ and $\boldsymbol{h}^{IT}(\boldsymbol{x}_t) = [h_1^{IT}(\boldsymbol{x}_t), \ldots, h_K^{IT}(\boldsymbol{x}_t]'$. The elements of $\boldsymbol{h}(\boldsymbol{x}_t)$ were defined in (9). We write the measurement equation as:

$$\boldsymbol{y}_t = \boldsymbol{h}(\boldsymbol{x}_t) + \boldsymbol{u}_t, \tag{23}$$

where the measurement error $\boldsymbol{u}_t$ is IID Normally distributed with mean zero. We assume that measurement errors are uncorrelated (across countries and maturities) and with variance that depends on the country but not on the yield maturity. The three measurement error standard deviations ω^0, ω^{GE} and ω^{IT} must be estimated with the other parameters.

The transition equation is given by

$$\boldsymbol{x}_{t+1} = \boldsymbol{\mu} + \boldsymbol{\Phi}\boldsymbol{x}_t + \boldsymbol{v}_t \tag{24}$$

where $\boldsymbol{v}_t \sim \mathcal{N}_{IID}(\mathbf{0}, \boldsymbol{\Sigma})$, and $\boldsymbol{\Sigma} = \boldsymbol{\Gamma}\boldsymbol{\Gamma}'$.

The measurement equation in (23) is nonlinear in the state variables. Therefore, we base quasi maximum likelihood inference on the Extended Kalman filter. Appendix A provides additional details on the estimation procedure.

4.2 Identification

To uniquely identify the latent states, we use an identification scheme similar to Dai and Singleton (2000) and impose $\boldsymbol{\Gamma} = \mathbf{I}_n$, $\boldsymbol{\delta}_1^0 \geq 0$, $\boldsymbol{\delta}_1^{GE} \geq 0$, $\boldsymbol{\delta}_1^{IT} \geq 0$, $\boldsymbol{\mu} = 0$ and $\boldsymbol{\Phi}^{\mathbb{Q}}$ lower triangular. This implies that the full parameter vector $\boldsymbol{\theta}$ is given by:

- δ_0^0, δ_0^{GE}, δ_0^{IT} (3 parameters),
- $\boldsymbol{\delta}_1^0$, $\boldsymbol{\delta}_1^{GE}$, $\boldsymbol{\delta}_1^{IT}$ ($n + 2n_0$ parameters),
- $\boldsymbol{\Phi}^{\mathbb{Q}}$ ($\frac{n(n+1)}{2} - n_{GE}n_{IT}$ parameters),
- $\boldsymbol{\mu}^{\mathbb{Q}}$ (n parameters),
- $\boldsymbol{\Phi}$ (n^2 parameters),
- ω^0, ω^{GE}, ω^{IT} (3 parameters)
- θ_1, θ_2, θ_3 (3 parameters)

for a total of $9+2n_0-n_{GE}n_{IT}+\frac{5n+3n^2}{2}$ parameters. For the specification selected in section 3.2, we have $n = 4$, $n_0 = 2$ and $n_{GE} = n_{IT} = 1$, implying a total of 46 parameters to be estimated.

We impose stationarity under $\mathbb{Q}$ by constraining the diagonal elements of $\boldsymbol{\Phi}^{\mathbb{Q}}$ between 0 and 1; we also impose stationarity under $\mathbb{P}$ by imposing that all the eigenvalues of $\boldsymbol{\Phi}$ are strictly smaller than 1.

Figure 4: Fit for selected maturities

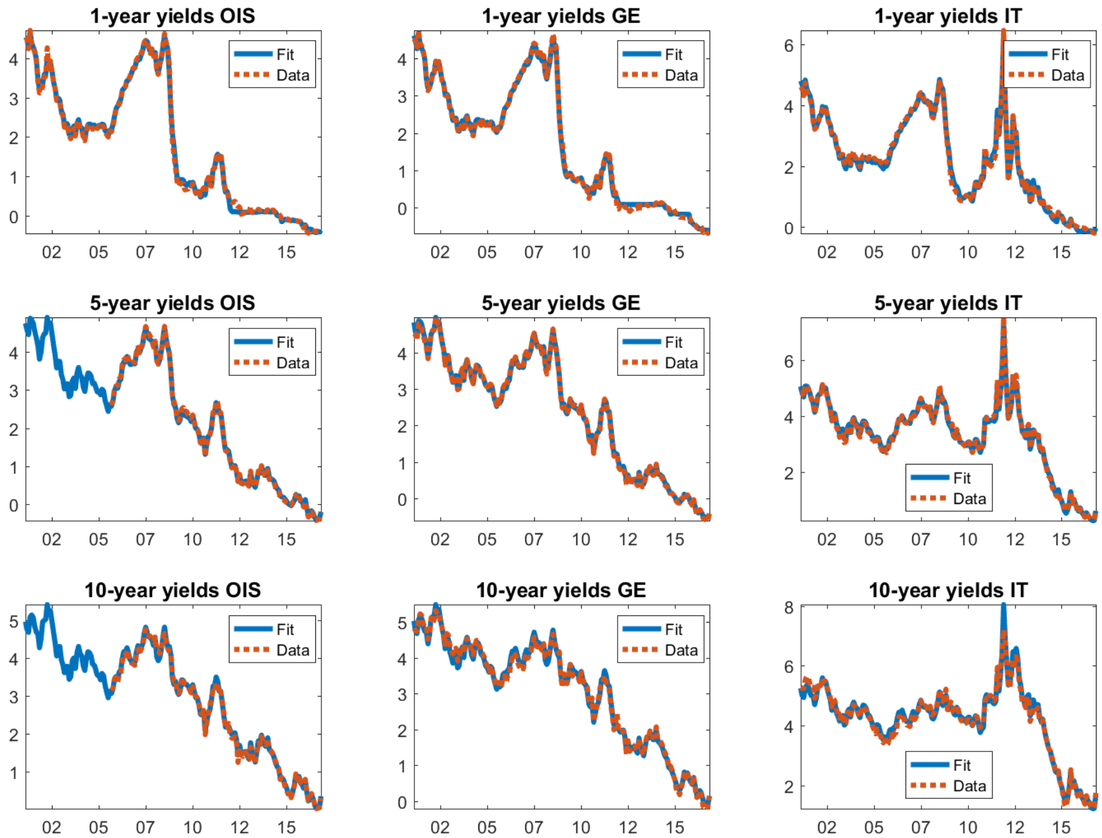

This figure reports observed and fitted yields with maturities 1-year (top plots), 5-year (middle plots), 10-year (bottom plots) for OIS (left plots), German (centre plots) and Italian (right plots) yields.

5 Results

We estimate the joint shadow rate term structure model for OIS, German and Italian yield curves using data from January 2001 to October 2016 by quasi-maximum likelihood and the Extended Kalman filter. In the next three subsection we present the model estimation results, the estimated shadow rates and shadow spreads, and the implications of the interest rate lower bound for the properties of sovereign spreads.

Table 4: Estimated parameters

$\boldsymbol{\mu}^{\mathbb{Q}}$	$\boldsymbol{\Phi}^{\mathbb{Q}}$			
-0.084*** (0.018)	0.994*** (0.001)	0	0	0
0.055 (0.093)	-0.044*** (0.006)	0.973*** (0.003)	0	0
0.109 (0.082)	-0.014 (0.018)	-0.015* (0.008)	1.000*** (0.000)	0
0.068*** (0.009)	0.000 (0.005)	-0.003 (0.003)	0	0.997*** (0.001)

θ	$\boldsymbol{\Phi}$			
0.090*** (0.012)	0.927*** (0.084)	-0.042 (0.032)	-0.017 (0.097)	-0.081 (0.055)
0.025 (0.03)	-0.050 (0.223)	0.927*** (0.081)	-0.002 (0.198)	-0.130 (0.157)
-0.220*** (0.057)	-0.155 (0.119)	-0.058 (0.04)	0.873*** (0.042)	-0.101* (0.058)
	-0.060 (0.124)	-0.012 (0.039)	-0.033 (0.127)	0.913*** (0.122)

δ_0	$\boldsymbol{\delta}_1^0$	$\boldsymbol{\delta}_1^{GE}$	$\boldsymbol{\delta}_1^{IT}$	ω
1.181*** (0.196)	0.000 (0.002)	0.012 (0.007)	0.073** (0.037)	0.084*** (0.004)
0.833*** (0.183)	0.221*** (0.019)	0.235*** (0.022)	0.268*** (0.04)	0.092*** (0.006)
1.232** (0.562)	0	0.044*** (0.007)	0	0.140*** (0.011)
	0	0	0.345*** (0.052)	

Note: this table reports the estimated parameters of the joint shadow rate term structure model for OIS, German and Italian yields. Asymptotic standard errors computed using the QML sandwich formula are reported in brackets. *, ** and *** denote significance at the 10%, 5% and 1% level.

5.1 Estimation results

Table 4 reports quasi maximum likelihood estimates of the parameters of our joint shadow rate model for risk-free, German and Italian term structures based on yields observed between January 2001 and October 2016. According to these estimates, the latent factors are less persistent under the actual probability measure $\mathbb{P}$ than under the risk-neutral measure $\mathbb{Q}$. The estimates of $\mathbf{\Phi}$ suggest that under $\mathbb{P}$ the German factor reacts negatively and significantly to an increase of the lagged Italian factor, without detecting a significant symmetric effect from the lagged German factor to the Italian one. The estimate of the shadow short rate parameters $\boldsymbol{\delta}_1^0$ suggests that the second common factor drives risk-free shadow short rates, and that the Italian factor has a stronger effect on the Italian shadow short rate than the German factor on the corresponding shadow short rate. The lower bound parameter is estimated to be positive and significant (even if small) in the first subperiod (θ_1), insignificant in the second subperiod (θ_2), and negative and significant in the last period (θ_3).

The fit of the model is in general good. In figure 4, we report the time series fit of the joint shadow rate term structure model for selected maturities. The figure indicates that the fit of the model is reasonable for OIS, German and Italian yields. The average yield curve fit, reported in figure 5, is also good for the three yield curves both in the full sample (from 2001 to 2016) and in the two half sub-samples (from 2001 to 2008 and from 2009 to 2016).

The root mean square errors (RMSE) in Table 5 indicate that the model has a slightly better fit for OIS and German yields than for Italian yields; this finding is in line with the preliminary analysis based on principal components outlined in section 3.2. The table also indicates that the performance of the model is slightly better in the first half of the sample with a RMSE of 0.090, compared with a RMSE 0.092 in the second half. Looking at each of the three yield curves, the table shows that the performance of the model actually improved in the second half of the sample for both OIS and German yields (that were more constrained by the lower bound), but it deteriorated for Italian yields. This may be due to the higher volatility of Italian yields after 2009 that is not entirely captured by the Italian factor. As for the performance across different maturities, the six month maturity has the largest RMSE for any sample and any yield curve.

In figure 6, we report the estimated factors. The top plot contains the updated estimates of the common risk-free factors provided by the Extended Kalman filter. The first common risk-free factor seems related to the inverse of the long term risk-free rate, while the second

Figure 5: Fitted yield curves

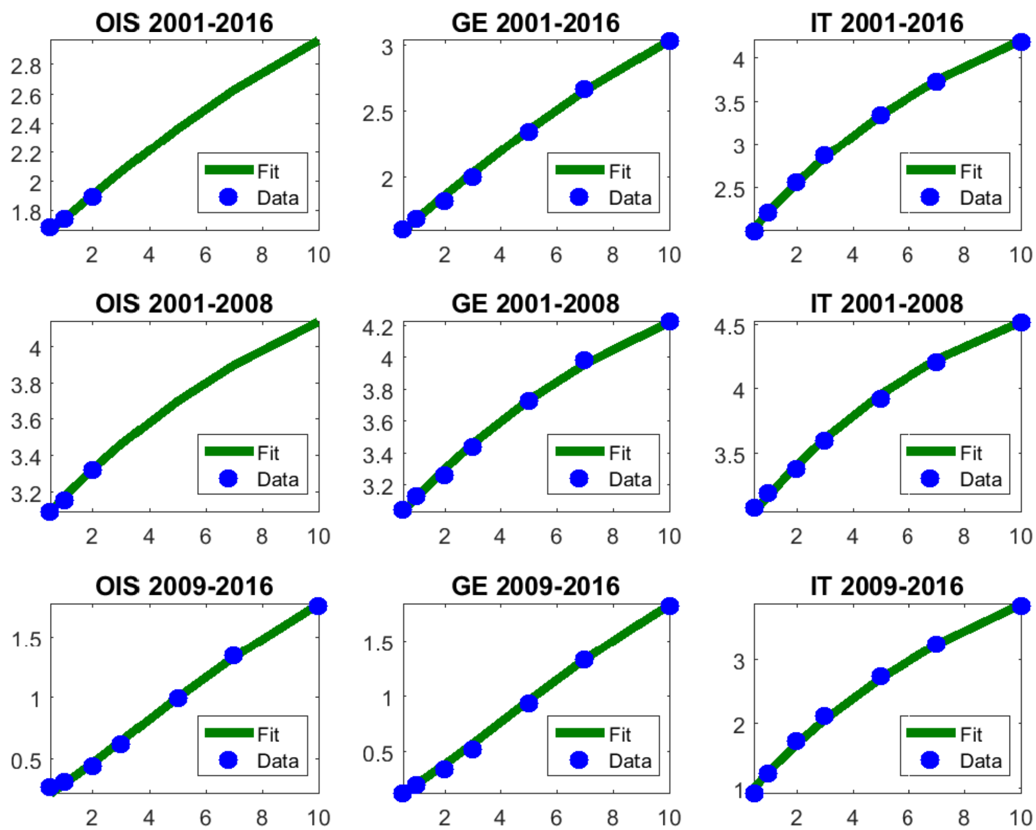

This figure reports average OIS, German and Italian yield curves on the full sample (top plot), first half sub-sample (middle plot) and last half sub-sample (bottom plot). The green lines refer to the model fit of the joint shadow rate term structure model and the blue dots refer to the observed data.

common factor is related to the short term risk-free rate. The Italian and German country factors reported in the bottom plot are related to the deviations of the Italian and German yield from the OIS rates. This is particularly evident for the Italian factor that spikes at the beginning of 2012. The figure also reveals the German factor steadily declines following the spike in the Italian factor, indicating a negative interaction between the German and the Italian factor, as anticipated in Table 4.

To illustrate how factors affect yields in the absence of a lower bound, in figure 7 we report the factor loadings of the shadow yields. The figure shows that the first common risk-free factor mainly loads on long term yields with a negative coefficient, while the second

Table 5: RMSE

Full sample 2001-2016								
	0.5	1	2	3	5	7	10	Average
OIS	0.112	0.070	0.085	0.073	0.044	0.038	0.067	0.070
GE	0.123	0.065	0.100	0.087	0.054	0.060	0.099	0.084
IT	0.213	0.098	0.119	0.125	0.086	0.075	0.135	0.122
Average	0.149	0.078	0.102	0.095	0.061	0.058	0.101	0.092

Subsample 2001-2008								
	0.5	1	2	3	5	7	10	Average
OIS	0.126	0.063	0.093	0.081	0.047	0.041	0.084	0.076
GE	0.148	0.055	0.115	0.090	0.055	0.066	0.114	0.092
IT	0.154	0.085	0.114	0.093	0.067	0.068	0.133	0.102
Average	0.143	0.067	0.107	0.088	0.056	0.058	0.110	0.090

Subsample 2009-2016								
	0.5	1	2	3	5	7	10	Average
OIS	0.096	0.077	0.076	0.069	0.042	0.037	0.059	0.065
GE	0.090	0.074	0.084	0.085	0.052	0.053	0.081	0.074
IT	0.259	0.110	0.123	0.150	0.101	0.083	0.138	0.138
Average	0.148	0.087	0.094	0.101	0.065	0.058	0.092	0.092

Note: this table reports root mean square error of the joint shadow rate term structure model for OIS, German and Italian yields on the full sample (top panel), the first half sub-sample (middle panel) and the last half sub-sample (bottom panel).

common risk-free factor has larger loadings on short term interest rates than on long term ones. The factor loadings on the common factors are similar for OIS and German shadow yields, and slightly different for the Italian shadow yields. This indicates that the country-specific component for Italian yields also depends on the risk-free factors. The German factor has a constant loading for all maturities, indicating that it shifts the whole German shadow yield curve. The Italian factor has large loadings for all maturities but slightly larger for shadow short yields, suggesting that this factor shifts the whole Italian shadow yield curve but shadow short rates are shifted slightly more.

In section 2.3, we decomposed observed yields into shadow yields and lower bound wedges, where the former are linear in the factors and the latter depend on the distance of the shadow forward rates from the lower bound and the volatility of future shadow rates under $\mathbb{Q}$. To

Figure 6: Latent factors

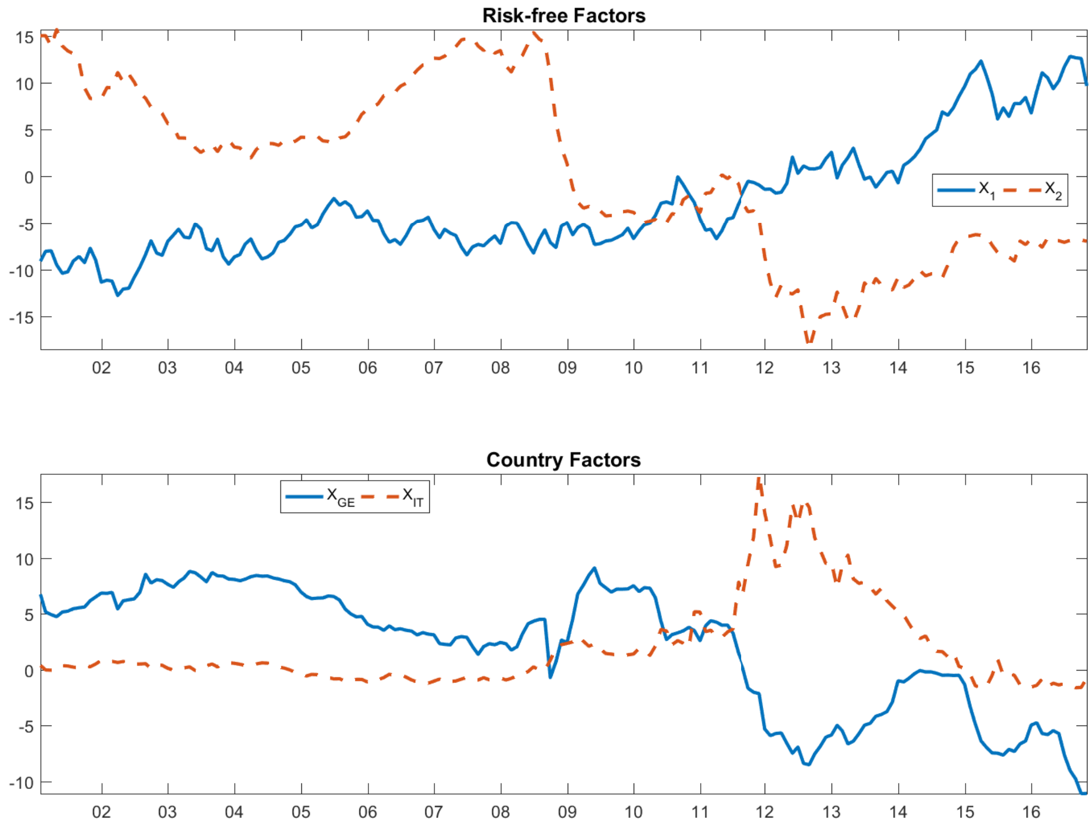

This figure reports the estimated common risk-free factors (top plot) and the estimated country-specific factors for Germany and Italy (bottom plot) of the joint shadow rate term structure model for OIS, German and Italian yields.

assess the magnitude of the lower bound wedge, we estimated σ_τ^i, the volatility under $\mathbb{Q}$ of future shadow rates as in equation (7) for the three term structures. Figure 8 plots the estimates with respect to the maturity τ. It is apparent that the estimated volatility for German and OIS future shadow rates is similar at all maturities, while the estimated Italian volatility is larger for all τ. This implies that for the same distance between shadow forward rates and the lower bound, Italian yields contain a larger lower bound wedge, see (13), (17) and figure 1.

Figure 7: Shadow yields factor loadings

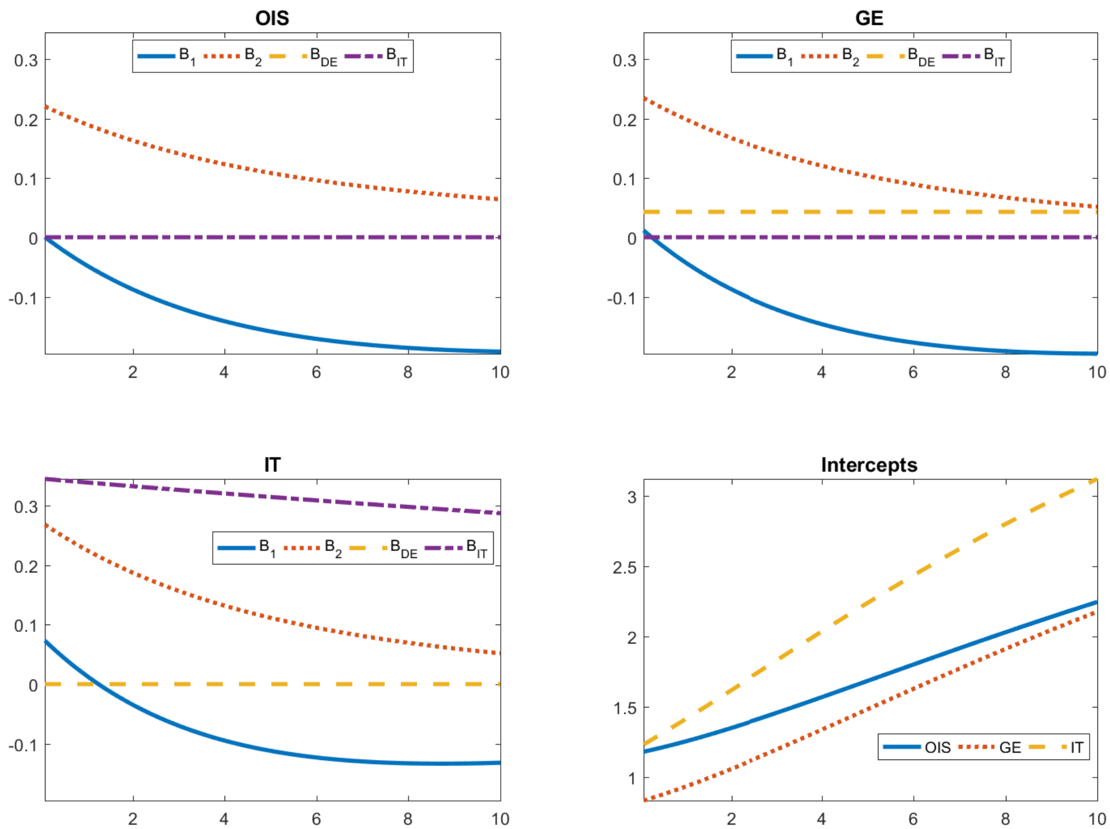

This figure reports the estimated shadow yields factor loadings in Equation (16) and obtained from the joint shadow rate term structure model for OIS, German and Italian yields.

5.2 Observed rates and shadow rates

To illustrate the effect of the lower bound on shadow yields, figure 9 reports OIS, German and Italian observed yield curves on two dates. The first date is April 2013, when OIS and German short rates were at the lower bound, but Italian rates were far from it. The second date is February 2015, when short term OIS and German yields were negative, and the six month Italian yield was close to the lower bound. In the figure, we report observed yields, fitted yields defined in (9) and shadow yields defined in (15). In April 2013, observed, fitted and shadow Italian yields coincided. Instead, shadow OIS and German yields were below the observed yields and negative for short maturities. In February 2015, shadow Italian yields

Figure 8: Forward rate volatility under the risk-neutral measure

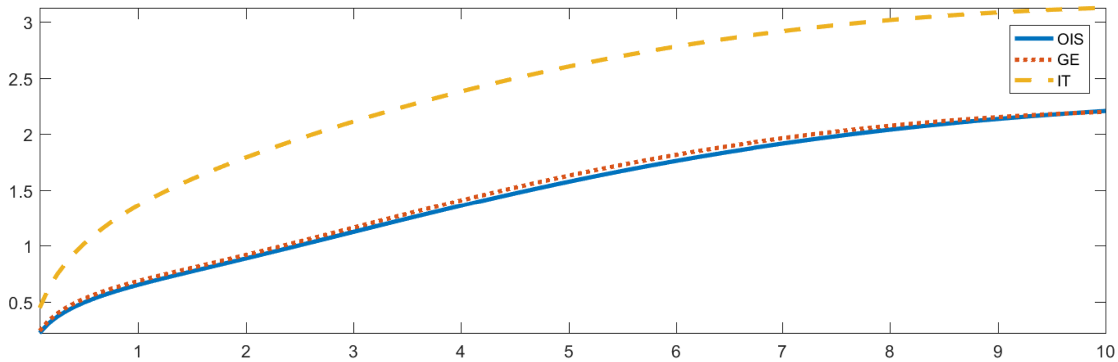

This figure reports the estimated forward rate volatility under the risk-neutral measure in Equation (7) obtained from the joint shadow rate term structure model for OIS, German and Italian yields.

were also below the observed yields, and negative for short rates. However, OIS and German shadow yields were negative for all maturities, indicating that, at this date, OIS and German lower bound wedges were large at any maturity. The figure also shows that our specification of a time-varying lower bound allows the lower bound to be close to zero in April 2013, and negative in February 2015.

In figure 10, we report the time series of the 10 year yields and shadow yields. The figure shows that, since mid-2011, the OIS and German 10 year shadow yields are lower than the observed yields. The Italian 10 year shadow yield becomes lower than the observed yield only by 2015. The time series plot of the lower bound wedges shows that OIS and German 10 year yields have been constrained by the lower bound since mid-2011 and that the effect of the constraint has been stronger on the German 10 year rate than on the OIS one. The figure also shows that the Italian lower bound wedge has been non-negligible also before the interest rates reached the lower bound. This can be explained by the large estimated Italian future shadow rates volatility under $\mathbb{Q}$, as shown in figure 8. The Italian lower bound wedge increases in 2014 and reaches the same level as the OIS lower bound wedge by the end of the sample.

Sovereign spreads, shadow spreads and spread wegdes are reported in figure 11. The figure indicates that the joint shadow rate term structure model for OIS, German and Italian yields fits well all 10 year spreads. We can also see that the 10 year German-OIS spread is smaller than the Italian-OIS and the Italian-German spreads in the sample period. As for the

Figure 9: Yield curves on two selected dates

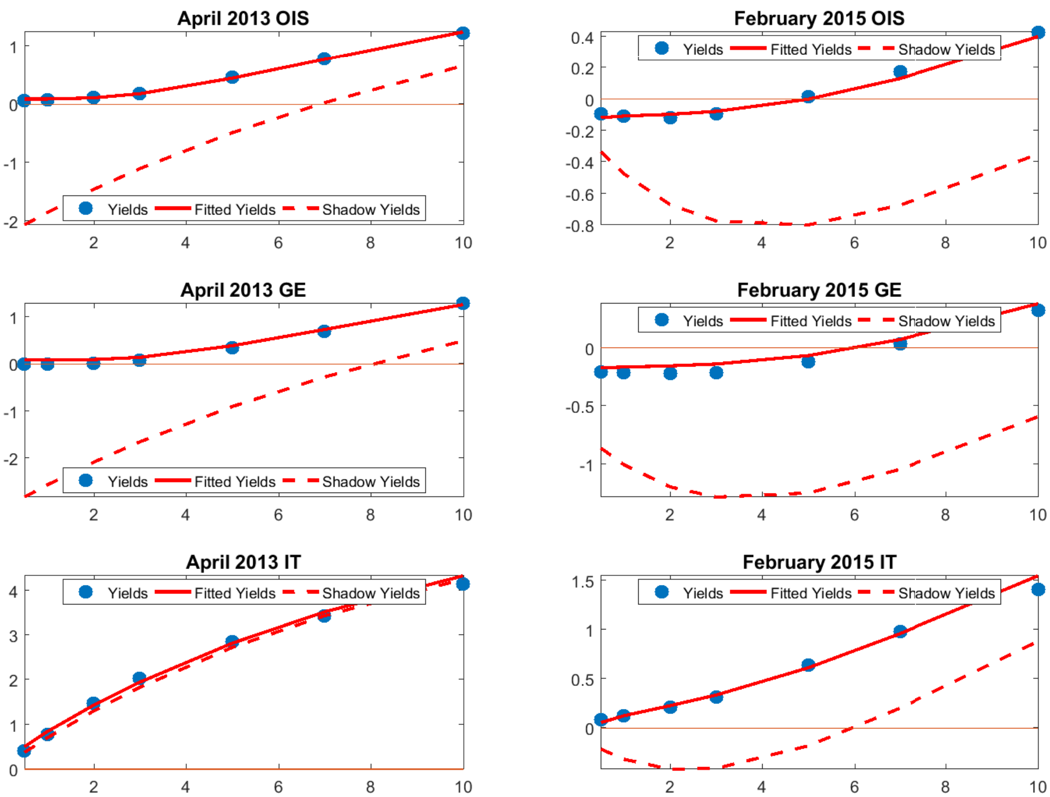

This figure reports OIS, German and Italian yield curves on two selected date: April 2013 (left plots) and February 2015 (right plots). The blue dots denote the observed yields, the red continuous line denotes the fitted yields defined in (9) and the dashed red line denotes the shadow yields defined in (15).

difference between observed spreads and shadow spreads, the figure shows that the German-OIS shadow spread is lower than the observed spread since mid-2011; on the contrary, during the same period the Italian-OIS and the Italian-German shadow spreads are larger than the corresponding observed spreads. The time series of the sovereign spread wedges, i.e. the nonlinear components of spreads, show that, when interest rates reached the lower bound, the German-OIS spread wedge became large and positive, while the Italian-OIS and the Italian-German spread wedges became large and negative. This is in line with our discussion in section 2.4 regarding the sign of the sovereign spread wedge and the presence of sovereign risk. The German-OIS sovereign spread wedge is positive because, due to the safety premium on German bonds, German short rates are closer to the lower bound, and thus more constrained

Figure 10: 10 year yields, shadow yields and lower bound wedges

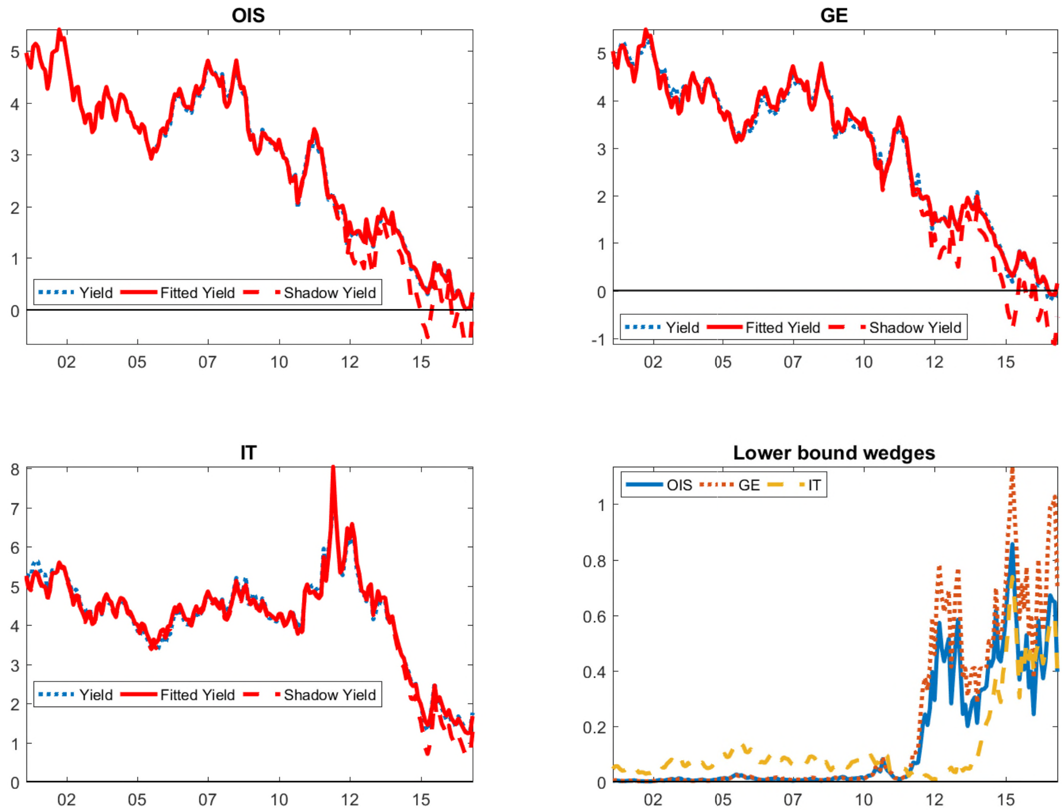

This figure reports 10 year yields, shadow yields and lower bound wedges for OIS, Germany and Italy. In the top plots and the bottom left plot, the blue line denotes observed yields, the red line denotes fitted yields as in (9) and the dashed red line denotes the shadow yields as in (15). The bottom right plot reports the lower bound wedges for the 10 year OIS, German and Italian yields, computed as in 17

than OIS rates. On the contrary, due to the presence of sovereign risk, Italian short rates are larger than OIS and German rates, which implies that they are less constrained by the lower bound. As a consequence, Italian-OIS and Italian-German spread wedges are negative. Summary statistics for the sovereign spread wedges, reported in Table 6, show that in our sample they reached the maximum of 0.38% for German-OIS spreads and the minimum of -0.564% and -0.775% for, respectively, Italian-OIS and Italian-German spreads.

Figure 11: 10 year spreads, shadow spreads and spread wedges

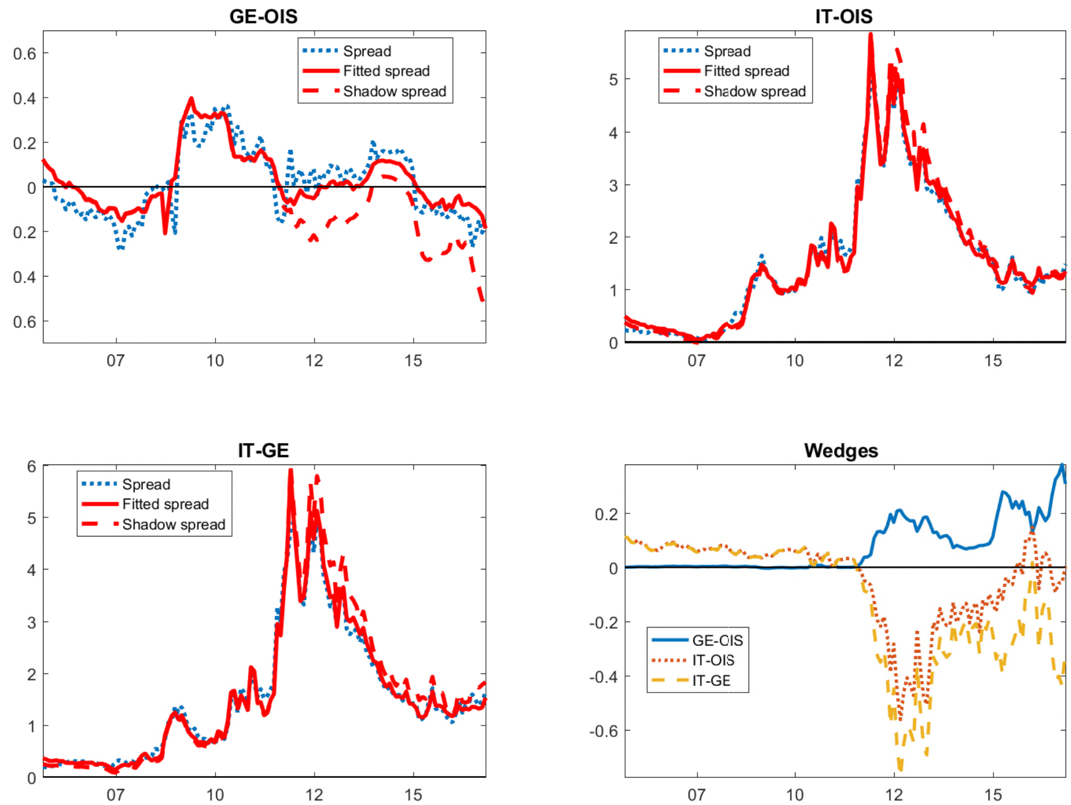

This figure reports 10 year spreads, shadow spreads and spread wedges for OIS, Germany and Italy. In the top plots and the bottom left plot, the blue line denotes observed spreads, the red line denotes fitted spreads and the dashed red line denotes the shadow spreads. The bottom right plot reports the lower bound spread wedges for the 10 year GE-OIS, IT-OIS and IT-GE spreads. Shadow spreads and lower bound spread wedges are computed as in (19).

5.3 Effects of the lower bound on sovereign spreads

The fact that sovereign spread wedges become non-negligible when term structures are close to the lower bound has three important implications for the properties of long term sovereign bond spreads at the interest rate lower bound.

First, the distribution of observed spreads becomes skewed as interest rates approach the lower bound. To assess this feature, for each date in the sample we simulated under the physical measure $\mathbb{P}$ 20,000 trajectories of the latent factors over a 12 month horizon, starting from their updated estimates obtained from the Extended Kalman filter. To save space,

Table 6: Summary statistics of Sovereign Spread Wedges

	Mean	Std	Min	Max	Q(25)	Q(75)
GE-OIS	0.075	0.096	-0.004	0.380	0.002	0.146
IT-OIS	-0.043	0.157	-0.564	0.149	-0.132	0.065
IT-GE	-0.119	0.224	-0.775	0.113	-0.297	0.062

Note: this table reports summary statistics for the 10 year sovereign spread wedges of Germany with respect to the OIS, Italy with respect to OIS, and Italy with respect to Germany.

Figure 12: Skewness of IT-GE Spread Distribution

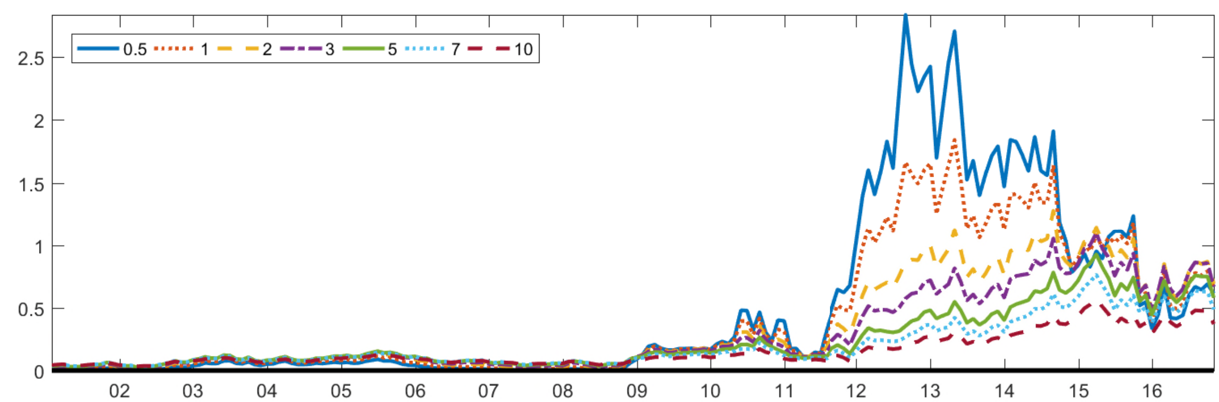

This figure reports the skewness index of the $\mathbb{P}$-distribution of 12-months ahead sovereign spreads of Italy with respect to Germany at the 7 observed maturities. In each point in time, we use the estimated parameters and factors to simulate 20,000 paths of factors 12-months ahead using (2). Then substituting in (9), we obtain 20,000 simulated yields 12-months ahead, from which we compute the asymmetry index.

we report results only for the spread between Italian and German yields at the 7 observed maturities. Figure 12 plots the skewness of the distribution of the 12-months ahead simulated spreads against the date at which the trajectories were started. If we compare this figure with figure 3, it is clear that the skewness is very sensitive to the distance of the short end of the term structure to the lower bound. Before 2009, when all interest rates were sufficiently far from the lower bound, the distribution of the simulated spreads was fairly symmetric, but things changed significantly after 2009, when rates approached the lower bound. Note that the 5% critical threshold for a two-sided z-test of the null of zero skewness is 0.034;

hence, the null of a symmetric distribution is rejected for all dates after 2009. It is also apparent that the skewness is more pronounced the shorter the maturity of the spread under consideration, but it is nonetheless significant also for the 10 year spread.[4]

A second implication of the interest rate lower bound on sovereign spreads is the following: as observed spreads depend on the distance from the lower bound, an exogenous change in the latter affects observed spreads, even if the sovereign risk does not change. Figure 13 illustrates this feature for the case of the spread between Italian and German 10 year yields. In the top plot, for each date in the sample, we report the difference between the counterfactual 10 year yields, obtained after a 20 basis points reduction in the lower bound, and the fitted yields. The effect of a change in the lower bound on the 10 year yields clearly changes after the short rates of each country reach the lower bound, 2009 for the German rate and 2012 for the Italian rate. Up to 2009, an exogenous 20 basis point decrease in the lower bound would not have any effect on the 10 year German yield, after this date the effect would be a decrease of the 10 year German rate by as much as 14 basis points. As for the Italian 10 year yield, an exogenous 20 basis point decrease in the lower bound would always have a negative effect on the yield. This is due to the large risk-neutral volatility of the shadow forward rates, reported in figure 7, that increases the option value of cash. However, the effect of an exogenous 20 basis point decrease in the lower bound on the Italian 10 year yield also becomes larger when short term Italian rates reach the lower bound.

In the bottom plot of figure 13, at each point in time, we report the difference between the counterfactual 10 year sovereign spread between Italian and German rates, obtained after a 20 basis points reduction in the lower bound, and the fitted 10 year spread between Italian and German rates. The effect of an exogenous 20 basis point decrease in the lower bound on the long term spread of Italian bonds with respect to German bonds changes around mid-2009. Up to that date, an exogenous 20 basis point decrease in the lower bound would decrease all spreads by roughly 1 basis point. After this date the effect changes sign and becomes much larger, as the same decrease in the lower bound would increase the spread between Italian and German yields by as much as 8 basis points. Notice that, as

[4]It might seem counterintuitive that the distribution of the 12-months ahead sovereign spreads of Italy with respect to Germany is skewed to the right, since in our sample the German term structure is always closer to the lower bound and this would suggest a left skewed distribution for the spreads. However, the skewness of the spread depends on the skewnesses of the yields, their volatilities and their coskewnesses. Accordingly, a positive skewness of the distribution of the 12-months ahead sovereign spreads of Italy with respect to Germany is due to larger volatilities of Italian rates.

Figure 13: Effect of a lower bound shift of -0.20%

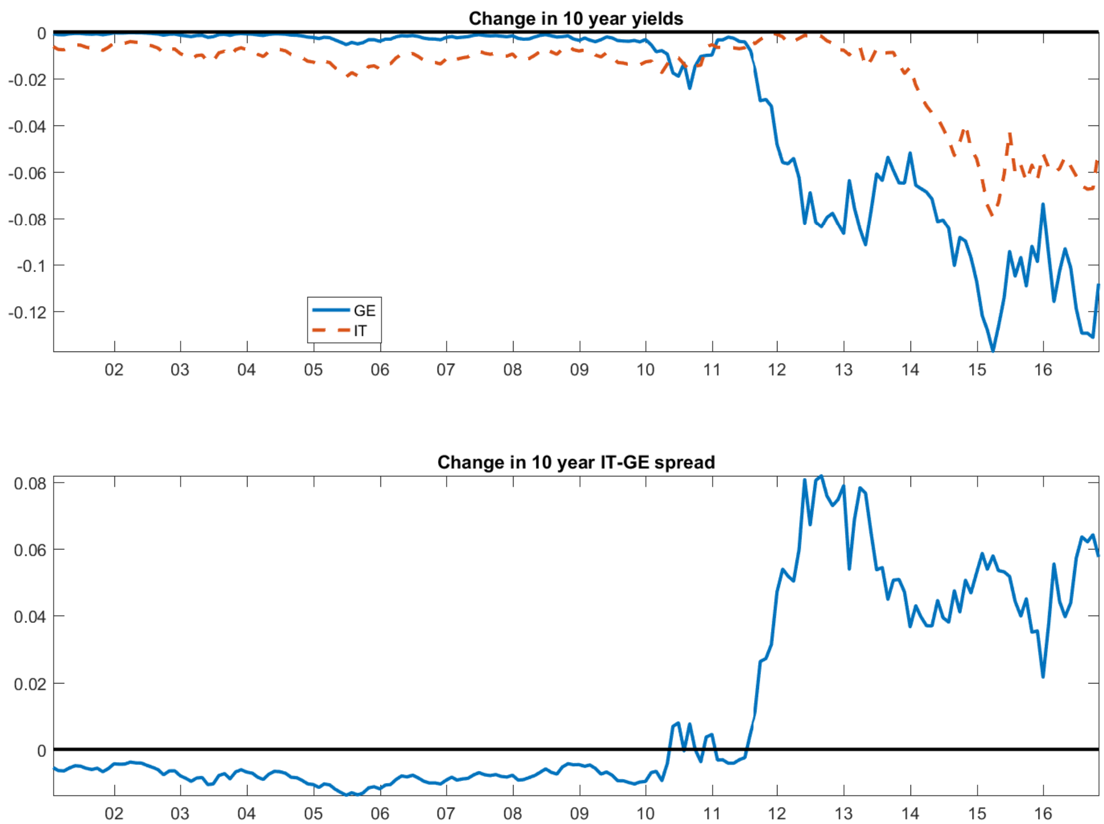

This figure reports the effects of a shift of the lower bound of -0.20% on the 10 year Italian and German yields (top plot) and on the 10 year IT-GE sovereign spread (bottom plot). In the top plot, at each point in time, we report the difference between the counterfactual 10 year yields (computed by lowering by 0.20% the lower bound in (9)) and the fitted yields. In the bottom plot, at each point in time, we report the difference between the counterfactual 10 year sovereign spread (computed from the counterfactual 10 year yields) and the fitted spread.

shown in (21), the lower bound depends on the deposit rate of the Eurosystem, which is a monetary policy instrument under the control of the European Central Bank. Therefore, results in figure 13 indicate that when short term rates are constrained by the lower bound, a monetary policy easing increases sovereign spreads, even if it does not affect the sovereign risk. This is due to the fact that the shift in the lower bound has a larger effect on rates that are closer to the bound.

A third and final implication of the existence of an interest rate lower bound on the prop-

Table 7: Sovereign Government bonds and Credit Default Swaps

Dependent variable	$\Delta_{t,10}^{IT,GE}$	$\tilde{\Delta}_{t,10}^{IT,GE}$
Constant	-0.12***	-0.23***
	(0.04)	(0.05)
$\text{CDS}_t^{IT,GE}\mathbb{I}_{t<1/2012}$	0.81***	0.92***
	(0.09)	(0.10)
$\text{CDS}_t^{IT,GE}\mathbb{I}_{t\geq 1/2012}$	0.66***	0.86***
	(0.10)	(0.10)
$\Delta_{t-1,10}^{IT,GE}$	0.55***	
	(0.06)	
$\tilde{\Delta}_{t-1,10}^{IT,GE}$		0.53***
		(0.06)
R^2	0.97	0.97
Wald	22.51***	1.90

Note: this table reports regression parameters of 10 year IT-GE bond spreads and shadow bond spreads on 10 year CDS spreads between Italy and Germany. HAC standard errors with 5 lags and Bartlett kernel are reported in brackets. *, ** and *** denote significance at the 10%, 5% and 1% level. The Wald test statistic refers to the test of equality of the coefficients on CDS spreads. The sample contains 106 observations, from January 2008 to October 2016.

erties of long term bond spreads is that, when the constraint is binding, the observed spread looses its informational content about the sovereign risk, but the shadow spread does not. To check this, we regress the 10 year observed and shadow bond spreads between Germany and Italy on the 10 year CDS spread between the two countries. Each regression allows for one lag of the dependent variable and also the CDS spread parameter to take different values in the periods before and after January 2012.[5] Table 7 illustrates the estimation results and also reports the Wald test statistic of the null of equal CDS spread slope in the two subperiods. All tests are computed using the robust HAC variance matrix. The yield spread

[5]The results presented are robust to changing the cut-off date to any date from August 2011 to December 2012, and also to excluding observations from October 2011 to August 2012 (the period in which the Italian bond market was subject to large volatility).

coefficient on CDS spreads decreases from 0.81 before January 2012 to 0.66 after the same date; the robust Wald test of equal slopes rejects the null at the 5% level. The shadow yield spread estimates provide a different conclusion: the two slope parameters are very similar and the robust Wald test fails to reject the null of equal slopes. Given these results, we conclude that the relation between the CDS spread and the shadow yield spread was not affected by the lower bound on interest rates. On the contrary, the relation between CDS spreads and the observed yield spread significantly changed after 2012, when German short term rates reached the lower bound.

6 Conclusion

This paper studies the effect of the interest rate lower bound on spreads between long term sovereign yields in the Euro area. We develop a joint shadow rate term structure model for three yield curves: the risk-free one associated to OIS rates, the German one and the Italian one. This framework allows us to model the nonlinear relation between sovereign spreads and sovereign risk when interest rates are close to the lower bound.

We show that any sovereign spread can be decomposed into a shadow spread and a sovereign spread wedge. The shadow spread is linear in the country-specific factor measuring sovereign risk and represents the distance between long term yields that would prevail in the absence of a lower bound. The sovereign spread wedge captures the nonlinearities that arise at the lower bound, and can be seen as a measure of the extent to which the lower bound on short term rates constrains the observed spread. In particular, the sovereign spread wedge depends on the distance of the two countries shadow forward rates from the lower bound, as well as on the volatilities of future short term shadow rates of the two countries under the risk-neutral probability. When short term rates are close to the lower bound, the sovereign spread wedge is large and, as a consequence, the observed spread becomes less informative about the sovereign risk.

We estimate the model on zero-coupon yields from the three term structures over the period January 2001 - October 2016 by Gaussian quasi maximum likelihood based on the Extended Kalman filter. Our results highlight the presence of strong nonlinearities in the behavior of long term sovereign spreads at the interest rate lower bound. In particular, in 2012 the nonlinear component reduces the observed 10-year Italian spread with respect to Germany by as much as 77 basis points with respect to the its shadow counterpart. This nonlinear behavior has three important implications on the properties of long term sovereign spreads. First, as short term interest rates approach the lower bound, the distribution of predicted long term sovereign bond spreads becomes significantly skewed. Second, at the interest rate lower bound, yields and spreads are affected by possibly exogenous changes in the lower bound, even if sovereign risk has not changed. Finally, when term structures are close to the lower bound, observed spreads do not fully reflect the market perception of the relative riskiness of sovereign bonds; on the contrary, shadow spreads provide a reliable picture of the sovereign risk embedded in observed term structures.

References

Andreasen, Martin M, and Andrew Meldrum (2015) 'Dynamic term structure models: The best way to enforce the zero lower bound in the united states.' *Bank of England Working Paper No. 550/2015*

Bauer, Michael D, and Glenn D Rudebusch (2016) 'Monetary policy expectations at the zero lower bound.' *Journal of Money, Credit and Banking* 48(7), 1439–1465

Black, Fischer (1995) 'Interest rates as options.' *The Journal of Finance* 50(5), 1371–1376

Carriero, Andrea, Sarah Mouabbi, and Elisabetta Vangelista (2016) 'Uk term structure decompositions at the zero lower bound.' *Document de travail - Banque de France N0. 589/2016*

Christensen, Jens HE, and Glenn D Rudebusch (2014) 'Estimating shadow-rate term structure models with near-zero yields.' *Journal of Financial Econometrics* 13(2), 226–259

—— (2016) 'Modeling yields at the zero lower bound: Are shadow rates the solution?' In 'Dynamic Factor Models' (Emerald Group Publishing Limited) pp. 75–125

Dai, Q., and K. Singleton (2000) 'Specification analysis of affine term structure models.' *Journal of Finance* 55, 1943–1978

Dawachter, Hans, Leonardo Iania, and Jean-Charles Wijnandts (2016) 'The response of euro area sovereign spreads to the ECB unconventional monetary policies.' Technical Report, National Bank of Belgium

Egorov, Alexei V, Haitao Li, and David Ng (2011) 'A tale of two yield curves: Modeling the joint term structure of dollar and euro interest rates.' *Journal of Econometrics* 162(1), 55–70

Ichiue, Hibiki, Yoichi Ueno et al. (2007) 'Equilibrium interest rate and the yield curve in a low interest rate environment.' *Bank of Japan Discussion Paper No.07-E-18/July 2007*

Kim, Don H, and Kenneth J Singleton (2012) 'Term structure models and the zero bound: an empirical investigation of japanese yields.' *Journal of Econometrics* 170(1), 32–49

Kim, Don H, and Marcel Priebsch (2013) 'Estimation of multi-factor shadow-rate term structure models.' *Board of Governors of the Federal Reserve System, Washington, DC, October*

Kortela, Tomi (2016) 'A shadow rate model with time-varying lower bound of interest rates.' *Bank of Finland Research Discussion Paper No. 19/2016*

Krippner, Leo (2012) 'Modifying gaussian term structure models when interest rates are near the zero lower bound.' *Reserve Bank of New Zealand Discussion Paper No. 2012/02*

——— (2013) 'A tractable framework for zero-lower-bound gaussian term structure models.' *CAMA Working Paper No. 49/2013*

Krippner, Leo (2015) *Zero Lower Bound Term Structure Modeling: A Practitioners Guide* (Palgrave Macmillan)

Lemke, Wolfgang, and Andreea L Vladu (2017) 'Below the zero lower bound: A shadow-rate term structure model for the euro area.' *Working Paper Series - European Central Bank No. 1991/2017*

Pericoli, Marcello, and Marco Taboga (2015) 'Understanding policy rates at the zero lower bound: insights from a bayesian shadow rate model.' *Bank of Italy Temi di Discussione (Working Paper) No. 1023/2015*

Piazzesi, Monika (2010) 'Affine term structure models.' *Handbook of financial econometrics* 1, 691–766

Ruge-Murcia, Francisco J (2006) 'The expectations hypothesis of the term structure when interest rates are close to zero.' *Journal of Monetary Economics* 53(7), 1409–1424

Swanson, Eric T, and John C Williams (2014) 'Measuring the effect of the zero lower bound on medium-and longer-term interest rates.' *The American Economic Review* pp. 3154–3185

Wu, Jing Cynthia, and Fan Dora Xia (2016) 'Measuring the macroeconomic impact of monetary policy at the zero lower bound.' *Journal of Money, Credit and Banking* 48(2-3), 253–291

—— (2017) 'Time-varying lower bound of interest rates in Europe.' Mimeo

A Estimation of the shadow rate term structure model

The state space representation of the shadow rate term structure model is

$$\begin{aligned}\boldsymbol{y}_t &= \boldsymbol{h}(\boldsymbol{x}_t) + \boldsymbol{u}_t, \quad \boldsymbol{u}_t \sim \mathcal{N}_{IID}(\mathbf{0}, \boldsymbol{\Omega})\\ \boldsymbol{x}_{t+1} &= \boldsymbol{\mu} + \boldsymbol{\Phi}\boldsymbol{x}_t + \boldsymbol{v}_t, \quad \boldsymbol{v}_t \sim \mathcal{N}_{IID}(\mathbf{0}, \boldsymbol{\Sigma}).\end{aligned}$$

where $\boldsymbol{\Sigma} = \boldsymbol{\Gamma}\boldsymbol{\Gamma}'$ and $\boldsymbol{\Omega}$ is diagonal with variances equal to $(\omega^0)^2$, $(\omega^{GE})^2$ and $(\omega^{IT})^2$ for measurement errors on OIS, German and Italian yields, respectively.

- We use a diffuse initialization of the Extended Kalman filter as follows

$$\widehat{\boldsymbol{x}}_{1|0} = \mathrm{E}(\boldsymbol{x}_1) = (\mathbf{I}_n - \boldsymbol{\Phi})^{-1}\boldsymbol{\mu}$$

  and

$$\mathbf{P}_{1|0} = \mathrm{E}[(\boldsymbol{x}_1 - \widehat{\boldsymbol{x}}_1)(\boldsymbol{x}_1 - \widehat{\boldsymbol{x}}_1)'] = 100\,\mathbf{I}_n$$

- The forecasts of the observables' values and their approximate MSEs are given by:

$$\widehat{\boldsymbol{y}}_{t|t-1} = \boldsymbol{h}(\widehat{\boldsymbol{x}}_{t|t-1}), \quad t = 1, \ldots, T$$

  and

$$\mathrm{E}[(\boldsymbol{y}_t - \widehat{\boldsymbol{y}}_{t|t-1})(\boldsymbol{y}_t - \widehat{\boldsymbol{y}}_{t|t-1})'] \approx \widehat{\mathbf{H}}'_{t|t-1}\mathbf{P}_{t|t-1}\widehat{\mathbf{H}}_{t|t-1} + \boldsymbol{\Omega}, \quad t = 1, \ldots, T,$$

where $\widehat{\mathbf{H}}_{t|t-1} = \mathbf{H}(\widehat{\boldsymbol{x}}_{t|t-1})$, and

$$\mathbf{H}(\boldsymbol{x}_t)' = \begin{bmatrix} \mathbf{H}^0(\boldsymbol{x}_t)' \\ \mathbf{H}^{GE}(\boldsymbol{x}_t)' \\ \mathbf{H}^{IT}(\boldsymbol{x}_t)' \end{bmatrix}$$

with

$$\mathbf{H}^i(\boldsymbol{x}_t)' = \begin{bmatrix} \partial h_1^i(\boldsymbol{x}_t)/\partial \boldsymbol{x}_t' \\ \vdots \\ \partial h_K^i(\boldsymbol{x}_t)/\partial \boldsymbol{x}_t' \end{bmatrix}, \text{ for } i = 0,\ GE,\ IT.$$

Since $g'(z) = N(z)$, we get

$$\frac{\partial h_j^i(\boldsymbol{x}_t)}{\partial \boldsymbol{x}_t} = \frac{1}{\tau}\left[\mathbb{I}_{\mathbb{R}_+}(s_t^i - \underline{r}_t)\boldsymbol{\delta}_1^i + \sum_{j=1}^{\tau-1} N\left(\frac{a_j^i + \boldsymbol{b}_j^{i\prime}\boldsymbol{x}_t^i - \underline{r}_t}{\sigma_j^i}\right)\boldsymbol{b}_j^i\right],\ i = 0, GE, IT$$

where $\mathbb{I}_{\mathbb{R}_+}(z) = 1$ if $z > 0$, and 0 otherwise.

- Given their forecasted values, the updated values of the state variables are computed as:

$$\widehat{\boldsymbol{x}}_{t|t} = \widehat{\boldsymbol{x}}_{t|t-1} + \mathbf{P}_{t|t-1}\widehat{\mathbf{H}}_{t|t-1}(\widehat{\mathbf{H}}_{t|t-1}'\mathbf{P}_{t|t-1}\widehat{\mathbf{H}}_{t|t-1} + \boldsymbol{\Omega})^{-1}(\boldsymbol{y}_t - \widehat{\boldsymbol{y}}_{t|t-1}), \quad t = 1, \ldots, T$$

and

$$\mathbf{P}_{t|t} = \mathbf{P}_{t|t-1} - \mathbf{P}_{t|t-1}\widehat{\mathbf{H}}_{t|t-1}(\widehat{\mathbf{H}}_{t|t-1}'\mathbf{P}_{t|t-1}\widehat{\mathbf{H}}_{t|t-1} + \boldsymbol{\Omega})^{-1}\widehat{\mathbf{H}}_{t|t-1}'\mathbf{P}_{t|t-1}, \quad t = 1, \ldots, T$$

- Given their updated values, the forecasted values of the state variables are computed as:

$$\widehat{\boldsymbol{x}}_{t+1|t} = \boldsymbol{\mu} + \boldsymbol{\Phi}\widehat{\boldsymbol{x}}_{t|t}, \quad t = 1, \ldots, T-1$$

and

$$\mathbf{P}_{t+1|t} = \boldsymbol{\Phi}\mathbf{P}_{t|t}\boldsymbol{\Phi}' + \boldsymbol{\Sigma}, \quad t = 1, \ldots, T-1$$

- Finally, the likelihood function is computed using the recursive factorization:

$$\boldsymbol{y}_t|\mathbf{Y}_{t-1} \sim \mathcal{N}(\widehat{\boldsymbol{y}}_{t|t-1}, \widehat{\mathbf{H}}_{t|t-1}'\mathbf{P}_{t|t-1}\widehat{\mathbf{H}}_{t|t-1} + \boldsymbol{\Omega}), \quad t = 2, \ldots, T.$$